Master's thesis

NTNU
Norwegian University of Science and Technology
Faculty of Natural Sciences
Department of Materials Science and Engineering

Martin Grimstad

Using Surplus Heat to Pre-Heat Carbon Anodes for Aluminium Electrolysis

Master's thesis in Chemical Engineering and Biotechnology
Supervisor: Kristian Etienne Einarsrud
Co-supervisor: Asbjørn Solheim
June 2019

NTNU
Norwegian University of
Science and Technology

Martin Grimstad

Using Surplus Heat to Pre-Heat Carbon Anodes for Aluminium Electrolysis

Master's thesis in Chemical Engineering and Biotechnology
Supervisor: Kristian Etienne Einarsrud
Co-supervisor: Asbjørn Solheim
June 2019

Norwegian University of Science and Technology
Faculty of Natural Sciences
Department of Materials Science and Engineering

NTNU
Norwegian University of
Science and Technology

Acknowledgement

Firstly, I would like to thank my supervisor Associate Professor Kristian Etienne Einarsrud and my co-supervisor, Chief Scientist in SINTEF Industry, Asbjørn Solheim for their guidance, great advices and all the time they have spent helping me with this work.

I would also like to thank Alcoa Mosjøen for giving me the opportunity to perform experiments during my master thesis. Their good advices and assistance have been greatly appreciated. In particular I would like to thank Kim Ronny Elstad, Nina Omdahl, and Ellen Myrvold.

The current work has been organised in HighEFF - Centre for an Energy Efficient and Competitive Industry for the Future, an 8 year Research Centre under the FME-scheme (Centre for Environment-friendly Energy Research, 257632/E20). Support from the centre is acknowledged.

The use of the X-ray laboratory at NTNU is acknowledged. The kind assistance of the laboratory from Ole Tore Buset is gratefully acknowledged.

I will also acknowledge SINTEF for the use of their laboratory facilities and preparations of the samples.

Finally, I would like to thank my family and my friends for their support during this work.

Abstract

The carbon anodes are consumed in the Hall-Héroult process and must be replaced on a regular basis. When a new anode is placed into the aluminium cell, the bath will immediately freeze on the bottom surface of the anode creating a frozen insulating layer. The anode replacement will reduce the current pick-up rate and cause disturbance to the electrical and thermal balance in the cell in the first few days after replacement.

Experiments to study the benefit of pre-heating carbon anodes were carried out in industrial scale aluminium cells at Alcoa Mosjøen in Norway. The carbon anodes were pre-heated using surplus heat from spent anode butts inside an insulated anode container before being placed into the aluminium cell. The experiments showed that the anode reached temperatures up to 150 °C near the core and a surface temperature above 250 °C using butts as heat source. These temperatures could save up to 0.018 kWh/kg Al. The current pick-up rate of the pre-heated anodes were monitored and compared to normal pick-up rates.

The formation of frozen bath underneath both pre-heated and normal anodes were observed. Different pre-heating time was used, and samples of the frozen bath were removed from the bottom surface of the anodes and analysed using a CT-machine. Experiments performed showed that the longer pre-heating time could reduce the formation of frozen bath underneath the anodes.

In addition, air velocity and temperatures were measured inside the cell using a pitot tube and thermocouples.

Sammendrag

Karbon anoder brukes opp i Hall-Héroult prosessen og må erstattes regelmessig. Når en ny anode blir plassert i aluminiumsovnen, vil badet umiddelbart fryse på undersiden av anoden og danne et fryst isolerende lag. Denne anodeskiftingen vil redusere strømopptaket og forårsake forstyrrelser til den elektriske og termiske balansen i ovnen i de første dagene etter skiftet.

Eksperimenter for å se på fordelene ved å forvarme karbon anoder ble utført på industriell skala på aluminiumsovner hos Alcoa Mosjøen i Norge. Karbon anodene ble forvarmet ved bruk av overskuddsvarme fra brukte anode butts inne i en isolert anodebeholder før de ble plassert inne i aluminumsovnen. Eksperimentene viste at anoden nådde temperaturer på opptil 150 °C nært sentrum av anoden og overflatetemperaturer på over 250 °C ved bruk av butts som varmekilde. Disse temperaturene kan spare opptil 0.018 kWh/kg Al. Strømopptaket til de forvarmede anodene ble målt og sammenlignet med vanlige strømopptak.

Dannelsen av påfryst bad under både forvarmede og vanlige anoder ble observert. Forskjellige forvarmingstider ble brukt og prøver av det påfryste badet ble fjernet fra undersiden av anodene og analysert med en CT-maskin. Forsøk som ble utført viste at lengre forvarmingstid kunne redusere mengden påfryst bad som ble dannet under anodene.

I tillegg ble lufthastigheten og temperaturen inne i ovnen målt ved bruk av pitotrør og termoelementer.

Contents

List of Tables

List of Figures

Chapter 1

Introduction

1.1 Aluminium electrolysis

Aluminium is the third most abundant mineral in earth's crust, after oxygen and silicon [1]. Since aluminium has a high chemical reactivity it is not found in a pure element state in nature. Aluminium is only found in combined forms like oxides and silicates. The only method that is used to produce aluminium on an industrial scale in today's production is through the Hall-Héroult process [1]. In the Hall-Héroult process, alumina (Al_2O_3) is dissolved in a electrolytic bath which mainly consists of cryolite (Na_3AlF_6). An electric current is then driven through the bath causing an electrochemical reaction. This produces liquid aluminium and CO_2 gas.

The Hall-Héroult process was invented independently in 1886 by Paul Héroult (France) and Charles Martin Hall (USA). Since the invention of the Hall-Héroult process, the essential principles of the process has remained the same, but the understanding and the operations of the electrolysis cells has improved a lot. The improvements has amongst other decreased the current consumption of the process from 20-25 kWh/kg Al produced for about 75 years ago down to 13-14 kWh/kg Al [1]. Today, the average energy consumption of a primary aluminium smelter is around 14.5 kWh/kg Al on world basis while the state-of-art aluminium smelters has a energy consumption of about 12.7 kWh/kg Al [1].

In order to further decrease the energy consumption of the Hall-Héroult process, it is important to understand the anode replacement activity for the aluminium cells better. In the Hall-Héroult process, the carbon anodes are consumed. Due to this continuous carbon consumption in the aluminium cell, the anode has to be replaced after 25-28 days. Depending on the size of the cell, an aluminium cell contains about 20-40 anodes. Therefore, an anode replacement activity in a cell is

performed every 1 to 3 days [1]. An aluminium plant with a cell voltage between 4 and 5 volts typically has about 150 and 450 cells in each potlines. There can then be multiple potlines in a plant.

After about 28 days, 75-80 % of the carbon anode has been consumed and it has to be replaced with a new anode. During the anode replacement activity, the anode is removed from the cell and placed in an anode container to cool down inside the hall before it is sent to recycling and used to make new anodes. The removed anodes are called butts and will have a temperature of about 900 °C when removed. A new anode is then placed in the spot of the removed anode. When the anode is placed into the cryolite bath, it has a temperature of about 10-20 °C, depending on the temperature inside the pot room. The cryolite bath, on the other hand, has a temperature between 940 and 970 °C [1]. The stability of the Hall-Héroult cell is highly affected by this anode change operations. The temperature difference between the newly inserted anode and the molten cryolite bath will cause disturbance to the cell. For instance, the temperature difference will cause a formation of a thick quenched layer of frozen cryolite to occur underneath the newly set anode which can freeze all the way down to the liquid metal. The formation of this layer is dependent on several factors such as bath temperature, position in the cell, cell stability, alumina concentration and distribution, etc.

To further decrease the energy consumption of the aluminium process it is possible to take advantage of the large heat waste from the production. About half of the energy supplied to the process in the form of electric work is lost as heat. A constant high energy waste heat source from the process is the butts. They have temperatures upwards 900 °C and are normally just placed in the plant to release their heat out in the pot room before they are recycled and used to make new anodes. This high energy heat can be used to pre-heat the new carbon anodes which are going to be placed into the bath. By utilising the waste heat from the butts, less energy would be needed to heat the anodes up to a desired operational temperature inside the cell. This is heat that needs to be taken from the bath.

In 2014, Norway produced 1 200 000 tonnes of aluminium which was 2.4 % of the worlds production that year [2]. If one assumes an energy consumption of 14.5 kWh per kilogram of aluminium produced, this results in a 17.4 TWh of energy needed just to produce the aluminium. The gross energy consumption for Norway in 2014 was 126.4 TWh. The production of aluminium in Norway would then stand for 13.8 % of the energy consumption [3]. On a world basis there was produced 64.3 million tonnes of aluminium in 2018 [4].

1.2 Objectives

In this master thesis, the focus will be on the pre-heating method of carbon anodes before they are placed into the electrolysis bath in the cell. The pre-heating will be performed by using surplus waste heat from the spend anode butts. The anode and the butts will be placed into an insulated container and heated for different amount of time. To better understand the impact from the anode change on the aluminium cell, the formation of frozen bath will also be investigated.

To fully understand the impact the pre-heating has on the production of aluminium, several experiments were performed at Alcoa Mosjøen on industrial scale aluminium cells. The advantage of performing the experiments at an industry scale is that the results are realistic in terms of the impact on the industry. The objectives for this work are:

- Investigate how different pre-heating temperatures on the carbon anode affects the electrolysis process and disturbance on the cell in the initial 48 hours after anode change.
- Investigate the formation of frozen bath underneath carbon anodes after insertion in the cell
- Given an estimate of how much energy the pre-heating process can save

Chapter 2 gives details about the Hall-Héroult process and anode production. Chapter 3 gives an overview of previous research that has been done on the subject. An introduction to the different heat transfer mechanisms is given in chapter 4. Chapter 5 gives details about the setup of the experiments and how they were performed. The results are presented in Chapter 6. Chapter 7 gives discussion regarding the results. Finally, chapter 8 gives the concluding remarks.

Chapter 2

The Hall-Héroult process

2.1 Aluminium electrolysis

The vast majority of the world's smelters produce aluminium using the Hall-Héroult process. The Hall-Héroult process was invented by the American Charles Martin Hall and the Frenchman Paul Héroult independently in 1886. In the Hall-Héroult process, liquid aluminium is produced through a electrolytic reduction of alumina (Al_2O_3) which has been dissolved in an electrolyte bath. The electrolytic bath mainly consists of molten cryolite (Na_3AlF_6) [1]. Cryolite is used in the electrolysis process because it has a unique capacity as a solvent of alumina [5]. An illustration of the electrolysis cell used in the Hall-Héroult process is shown in Figure 2.1. At the cathode, AlF_3 is reduced to aluminium in a liquid state:

$$AlF_3 + 3\,Na^+ + 3\,e^- \rightarrow Al(l) + 3\,NaF \tag{2.1}$$

AlF_3 here presents the different complexes which contains aluminium, such as AlF_4^- and AlF_6^{3-} [6]. Due to the aluminium having a higher density than the cryolite, the liquid aluminium will fall to the bottom of the cell. In the Hall-Héroult process, the anodes are made of carbon, and one carbon anode typically weights between 1 and 1.3 tonnes. These carbon anodes are placed into the electrolytic bath. From the alumina, oxygen is discharged electrolytically and forming an intermediate product underneath the anode. Immediately after the oxygen is adsorbed onto the anodes, it reacts with the carbon and produces gaseous carbon dioxide (CO_2).

$$\frac{1}{2}\,Al_2O_3 + \frac{3}{4}\,C + 3\,NaF \rightarrow AlF_3 + \frac{3}{4}\,CO_2(g) + 3\,Na^+ + 3\,e^- \tag{2.2}$$

Combining the reaction the reaction occurring on the cathode and on the anode, Eq. 2.1 and 2.2, we get the following total reaction for the aluminium electrolysis [6]:

$$\frac{1}{2}\,Al_2O_3(\text{diss}\cdot) + \frac{3}{4}\,C(s) \rightarrow Al(l) + \frac{3}{4}\,CO_2(g) \tag{2.3}$$

where diss. is the dissolved alumina and s is the solid carbon in the anodes. To maintain the desired heat balance in the cell, a layer of alumina and frozen bath is added to the top of the bath and the anodes. This frozen layer, called the crust, will help to preserve the heat inside the cell and significantly reduce the oxidation of carbon anodes in air.

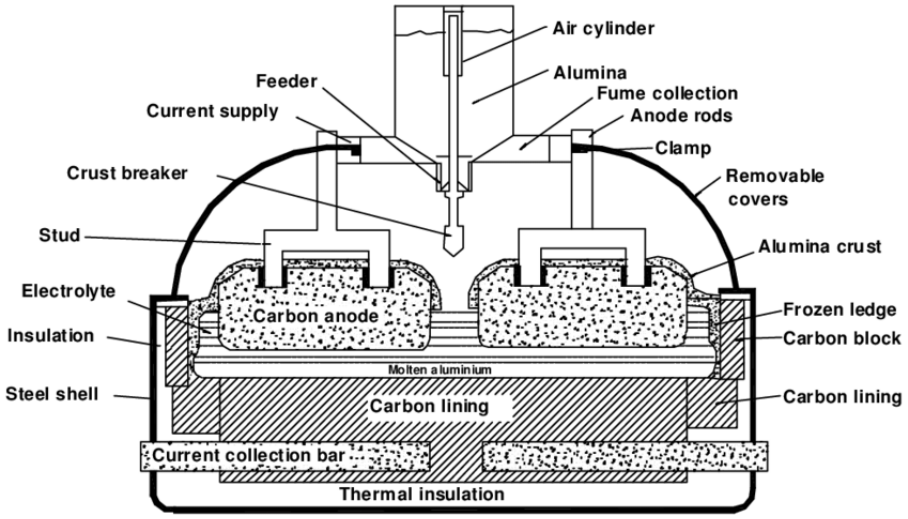

Figure 2.1: A cross-section of the Hall-Héroult aluminium electrolysis cell [7].

Inside the electrolysis cell during cell operation, the temperature on the cryolite bath is in general between 940 °C and 970 °C. Pure bath of cryolite will have a melting point of 1011 °C, so to lower the melting point, the liquidus temperature, different additives such as aluminium fluoride (AlF_3) and calcium fluoride (CaF_2) is added to the bath [8]. The electrolyte is not consumed in the electrolytic process, but due to hydrolysis, vaporization, and penetration of the cathode lining some electrolyte will be lost over time [5]. The electrolyte level is daily inspected by the operators and if necessary, the electrolyte is exchanged between the electrolysis cells.

The Hall-Héroult process requires a lot of energy to produce aluminium. The theoretical energy consumption from the process can be calculated using Equation 2.4.

$$W_{el} = \frac{U \cdot F \cdot |\eta_e|}{3600 \cdot M_{Al} \cdot X_{Al} \cdot \eta_{Al}} \tag{2.4}$$

Here, W_{el} is the energy consumed in the process per kilogram of aluminium produced given in kWh/kg Al, U is the applied cell voltage, F is Faraday's constant, η_e and η_{Al} is the stoichiometric number of electron and aluminium from Eq. 2.3, M_{Al} is the molar mass of aluminium, and X_{Al} is the current efficiency. The current efficiency is a ratio of how much aluminium which is made compared to how much it is theoretically possible to produce. The average industrial current efficiency for today's aluminium cells is typically in the range of 92-96 % [6].

Equation 2.4 can be simplified further. The equation contains only two variables, the applied cell voltage and the current efficiency. One then get the following simplified equation [1]:

$$W_{el} = \frac{2.9806 \cdot U}{X_{Al}} \tag{2.5}$$

The reversible voltage for the process is 1.2 V [1]. This is the theoretical minimum voltage that needs to be applied to the system for the reaction to occur. Due to several resistances in the cell, such as resistances in the bath, the anodes, and the cathode, and ohmic losses, the total cell voltage for an aluminium cell is typically in the range of 4.0-4.5 V. The main reason for a larger overvoltage is due to the resistance in the electrolyte bath. This voltage loss account for about 1.3 to 2.0 V which is due to the ohmic resistance in the bath [1].

To produce one tonne of aluminium, a theoretical amount of 334 kg of carbon is required [9]. The average real consumption of carbon in the electrolysis process is however at about 415 kg of carbon per tonne of aluminium. The additional consumption of carbon in the process is mainly due to the back reaction, air burn, and the Boudouard reaction. The back reaction, shown in Equation 2.6, is assumed to proceed via dissolved metal and dissolved carbon dioxide [1]. The chemical reaction is assumed to be instantaneous. As a result from the back reaction, more carbon is needed in the total reaction, Equation 2.3, to compensate for the aluminium lost. The back reaction, Equation 2.6, is the main reason for the loss in current efficiency, the ratio of how much aluminium that is produced compared to the theoretical amount of aluminium that can be produced according to the Faraday equation.

$$\mathrm{Al_{(diss.)}} + \frac{3}{2}\,\mathrm{CO_{2(diss.)}} \rightarrow \frac{1}{2}\,\mathrm{Al_2O_{3(diss.)}} + \frac{3}{2}\,\mathrm{CO_{(g)}} \tag{2.6}$$

To calculate the total amount of material from an electrochemical reaction produced on an electrode related to the total amount of charge passing through,

Faraday's law of electrolysis can be applied. The following laws presented in Grjotheim et. al [1] will apply for the amount of product formed at the electrode:

1. "The amount of product formed at each electrode will be proportional to the number of coulombs passing through the cell."

2. "The amount of each electrode product will be proportional to the equivalent mass of the product."

By applying the Faraday's law of electrolysis to the production of aluminium through the Hall-Héroult process, Equation 2.3, one gets:

$$m_{Al} = \frac{M_{Al} \cdot I \cdot t}{z \cdot F} \tag{2.7}$$

where m_{Al} is the theoretical amount of aluminium produced, M_{Al} is the molar mass of aluminium, I is the current, t is the time, z is the number of electrons in the electrode reaction, and F is Faraday's constant (96485 C/mol). Equation 2.7 can then be used to calculate the amount of material produced through an electrochemical reaction.

A few examples of situations where the current distribution to the anodes is in imbalance within the aluminium cell is shown in Figure 2.2 [10]. Depending on the size of the cell there will be 3 to 6 feeders for alumina. The distance between the anodes and the feeder can have an impact on the process, as shown in (a) and (c) in Figure 2.2. Alumina is added in relatively small amounts of between 1 and 5 kg in a periodical schedule [11]. The concentration of alumina in the bath close to the feeders can be higher compared to the concentration further away from the feeders, depending on how well the alumina is moved around in the bath. During the anode change, the temperature in the bath around a newly set anode might be reduced due to the low temperature of the new anode. If this anode is close to any of the feeders in the cell this can cause a decrease in the superheat which results in a reduced dissolution of alumina. Situation (b) shows the freezing of molten cryolite in relation to the anode change process. Since the anode has a low temperature between 5 °C and 20 °C when placed in the bath which has a temperature between 940 °C and 970 °C, this causes the molten cryolite to reach a temperature below its freezing point and the space between the new anode and the metal pad to freeze. Situation (d) and (e) shows the distance between the anode and the metal pad. The distance typically lays between 3 and 5 cm [1]. If the distance gets to large, the resistance in the bath will significantly increase and more voltage is needed to produce aluminium. If the distance gets too short there is a risk of short circuit if the anode gets in contact with the metal.

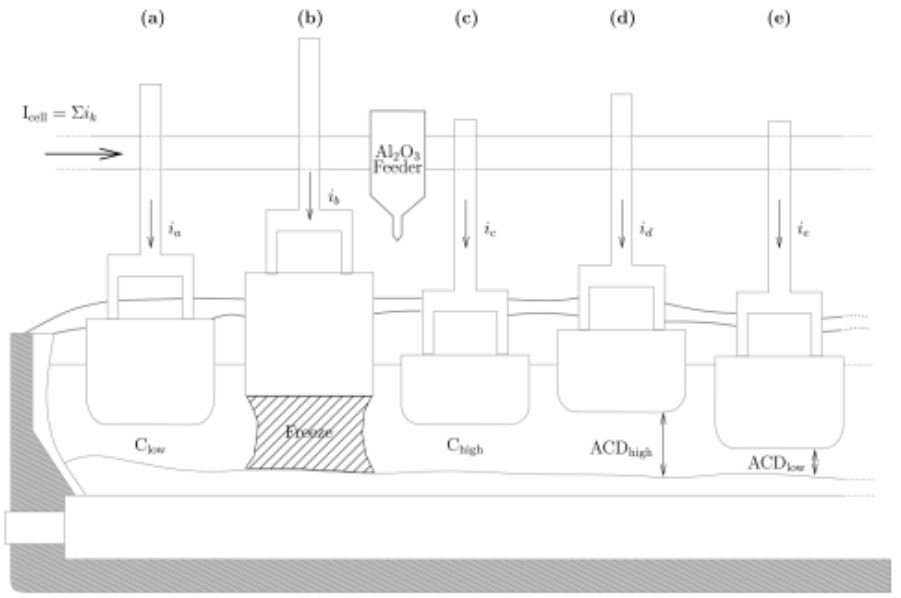

Figure 2.2: The figure shows some of the common local conditions that might affect the current distribution in the carbon anodes in an aluminium cell [10].

2.2 Carbon anode

The anodes are the source of carbon for the aluminium process. There are two different designs for the anodes, the prebaked anode and the Söderberg anode. The prebaked anodes are first moulded into shapes of blocks and then baked in an anode baking furnace. On top of the anode, iron studs which are connected to an aluminium rod are cast into the stub holes of the anode block. When the anode is placed into the cell, the rod and the studs will conduct the electric current to the anode [12]. The prebaked anodes are typically made from a mixture of 65 wt% calcined petroleum coke, 20 wt% recycled butts and 15 wt% coal tar pitch [9]. A good consistency and quality of the carbon products is important for the aluminium process. In the anode production one cannot compensate later for mistakes that was made at an earlier stage [13]. If the quality of the raw materials does not satisfy the need, the paste plant or the anode baking section cannot compensate for the deficiency.

The Söderberg anodes are continuous and self-baking [14]. This removes the costs of the forming, baking, and post-treatment of the anodes which comes with the prebaked anodes. The anodes used in the Söderberg process are made into briquettes made of petroleum coke and coal tar pitch, but the pitch binder content

is about 25 wt% to make sure the paste has the adequate flow of paste [12]. The briquettes are added on top of the anode and will soften due to the heat from the cell. As the bottom of the anode is consumed, the paste will move slowly down inside a steel casting towards the electrolyte. The paste is then baked as it travels further down. A large drawback to the Söderberg anodes is the high pitch content and the open top. The pitch content can cause the formation of polycyclic aromatic hydrocarbons (PAHs) which is a hazardous gas and combined with the open top can lead to a hazardous environment for the workers in the pot rooms.

For the anodes to meet the high demands to be used in the aluminium process, several requirements have to be fulfilled. Some of the requirements are high chemical purity, high electrical conductivity, high mechanical strength, and chemical homogeneity [1]. Since the Söderberg anodes are of a poorer quality than the prebaked anodes, they will also produce more unwanted carbon dust [15].

2.2.1 Forming

For the prebaked anodes, they are formed using either vibratory compacting or pressure moulding. Considering the quality of the anodes for each process, both processes will produce equally good anodes but to optimise the quality of the anodes the anode recipe has to be adapted to the forming process which is used [13].

For the pressure moulding, the paste needs to be cooled down to a temperature below the softening point of the pitch, about 5 to 10 °C below. The pitch is then filled into the anode mould and a pressure of about 35 MPa is applied to both the top and the bottom of the anode [16]. The density of the produced anodes will be approximately 1.6 kg/m^3 [1].

The other alternative to produce pre-baked anodes are by using the vibratory compacting method. The method is popular to use on large sized anodes. The anode paste will have a temperature of about 150 °C when placed into the mould and the top is then sealed. In some cases, a negative pressure of 0.1 to 0.3 bar is applied using a vacuum pump. The top is compressed with a pressure of about 3 to 15 MPa [12]. The vibration frequency is between 15 and 30 Hz. The formed anode then must be cooled down and this is typically done by placing them into a water bath spraying them with water. Producing the anode through vibratory compacting has a few advantages compared to the pressure moulding method. Using vibratory compacting, the anodes can be formed at a higher temperature without problems from the evaporating gases since they will be “shaken” out from the bulk [16].

2.2.2 Baking

The anode baking furnaces which are used for large scale anode baking in today's production are called ring furnaces. In the ring furnaces, the anodes are baked through high-temperature indirect heating by burning natural gas such as propane. There are two different ring furnaces which are used for producing carbon anodes for aluminium production, open ring top furnace and closed ring top furnace. In today's production, the open ring furnace is considered to be the state-of-the-art for baking of carbon anodes [13].

In the open top ring furnace, the anodes are stacked in chambers which are approximately 5 meters high, 5 meters long, and 1 meter wide. Each heating-section consists of up to four of these rectangular pits. The pits storing the anodes are separated by heating flue walls. The remaining space inside these pits are filled with granular coke to provide heat transfer to the carbon anodes from the flue walls and protect the anodes from oxidation [12]. Above 400 °C, the oxygen can react with carbon and produce CO_2. Inside the flue walls, the heat that has been produced from the combustion of the natural gas is transferred. The anodes will go through several physico-chemical changes during the whole baking process. The general changes that occurs for the anodes are mentioned here:

The first step in the baking process happens up to 200 °C. The pitch, which is used as a binder in the anodes, will expand as the temperature is increased. This thermal expansion will release any possible tension that might have been created at an earlier stage of the process. This expansion will also cause a reduction in the density of the anodes. Between 150 °C and 350 °C the pitch will start to redistribute into voids because of the pitch expansion. In this step, the mechanical strength, resistivity, and the permeability will be affected. There is also a risk of shape damage during this step. From 350 °C to 450 °C a minor reduction in the density will occur since volatiles of the light binder are released at this temperature. A transition from plastic to solid matrix will happen in the cooking part between 450 °C and 600 °C. Dilatometric changes could also occur due to the contractions and expansions within the anode block from the thermal gradients. Additionally, more volatiles will be released from the anodes. From 600 °C to 900 °C the post-coking happens. Heavy cracked volatiles such as methane (CH_4) and hydrogen gas (H_2) is released. The last heating step in the heat process reaches a temperature of up to 1200 °C. Here, reorientation of the crystalline and growth of the binder.

2.3 Energy balance in the electrolysis cell

The heat balance for the Hall-Héroult cell is a major concern in the process [1]. Due to the increased energy cost compared to other manufacturing costs and a larger environmental awareness, the modern cells are now built to preserve more of the heat produced in the process. Some of the produced heat from the process is needed to keep the molten aluminium and the bath at a correct temperature and heating the carbon anodes and the alumina, but this only accounts for about 20 % of the produced heat. The rest of the heat is lost to the surrounding air inside the aluminium plant.

The parameters that are responsible for the generation of heat inside the cell are the current density and the interpolar distance. For an operating cell, the cell design, thermal insulation, anode size and amperage will be given. The loss of heat in the cell will therefore be given by the cell voltage, or the interpolar distance in practice. The technology found in today's aluminium cells has made it possible to reduce the interpolar distance down to about 2.5-3 cm for the state-of-art smelters [17]. A lower distance would increase the risk of short-circuiting and the back-reaction which would cause a reduction in current efficiency.

The reduction in heat loss from the cells has been improved over the years. A good isolation is needed at certain areas of the cell to maintain a correct heat balance in the cell. Over time, this will save energy and increase the lifetime of the cell. The design of the cell needs to be in such a way that the correct bath temperature is maintained simultaneously as the heat flow over the side walls needs to be sufficient to maintain the frozen electrolyte on the side ledge to protect the walls of the cell and the outer edge of the cathode bottom. If the bottom of the cell were to be insufficiently insulated, this would lead to more heating leaving the cell and a thicker frozen bath will cover the cathode causing an increase in the cell voltage since the metal circulation pattern is disturbed. Contrarily, an excess of insulation would result in a too high temperature inside the cell, preventing the frozen bath to be formed on the side walls. Ultimately, this may result in erosion of the walls and cause an early side-lining failure. The top of the anodes and the bath is also covered in a crust of frozen bath and alumina, as can be seen in Figure 2.1 [18].

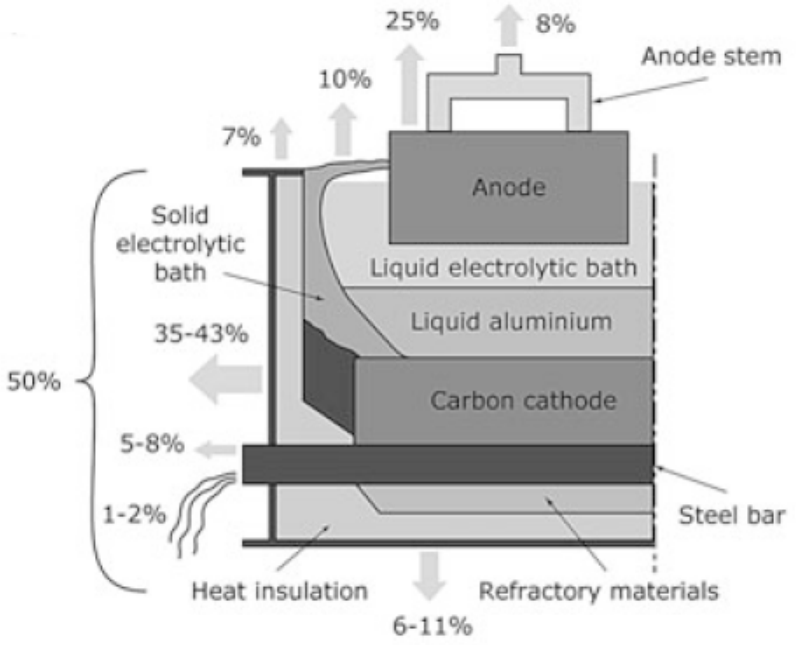

.

Figure 2.3: An illustration of the approximate heat loss from a Hall-Héroult cell divided into areas [19], [1]

Figure 2.3 shows a presentation of the heat loss from a Hall-Héroult in percent. The main heat loss is through the upper part of the cell. In the figure, the top includes the anodes, the stubs, and the crust that is covering the anodes and the bath. The alumina ore which is used to cover the anodes and the crust has a large potential for saving energy.

Since there is produced about 64.3 million tonnes of aluminium world-wide in 2019 and the process has such a large amount of waste heat, being able to utilise some of the waste heat could benefit the energy consumption of the process and reduce the environmental impact and reduce the expenses from the process.

Chapter 3

Literature review

Pre-heating of carbon anodes has been proven to be beneficial for the Hall-Héroult process. Jassim et al. [20] investigated how the pre-heating of anodes would affect the current pick-up rate of the process. The anodes had on average a temperature of 300 °C with a $\pm$ 11 % variation when they were placed in the cell. The anodes were heated using a gas pre-heated station which were able to pre-heat the anodes to a temperature between 470 °C and 500 °C. The experiments were performed on a total of 8 anodes on different position in an aluminium cell. They found that the pre-heated anodes would on average experience a 42 % faster evolution in current in the initial 6 hours after they were placed into the cell. A higher initial anode temperature and lower extracted energy from the molten electrolyte gave a better local superheat and mixing conditions for the electrolyte.

Similar to the study done by Jassim et al., done by Fortini et al. [21] investigated the effect pre-heating of anodes would have on the aluminium electrolysis. A pre-heating station was built which was capable of pre-heating up to six anodes per day to a temperature of 600 °C. Before being placed into the bath, the bottom of the anodes was heated up to a temperature between 484 °C and 512 °C. The studied showed that the pre-heating would have an improved electrical current pick up by the anodes immediately after placed into the bath. They study reported an increase of between 0.5 and 1 % in current efficiency. The anodes would also have significantly less frozen bath underneath it 2 hours after set. The anodes pre-heated to a temperature of 500 °C had no frozen bath after 2 hours while the anodes which had a temperature of 300 °C during insertion had some frozen bath underneath after 2 hours.

In 2019, a study by Picard et al. [22] was published where the formation of the frozen layer of molten cryolite which occurs in connection with the insertion of a new anode into the bath was investigated. In the study, the temperature and voltage drop evolutions were measured for sixteen selected anodes, while the frozen layer thickness were estimated through an image analysis after the anodes were removed from the aluminium cells. The amount of time the anodes spent inside the cell before they were removed were between 15 and 360 min. They found that the frozen layer of molten cryolite melted at a rate of about 0.000008-0.00001 m^3/min, and after 180 minutes the layer was completely melted. The study also conclude with that the frozen layer does not impact on the voltage drop but rather the temperature evolution. After 120-150 minutes the heating rate of the anode changed. This is within the time where the frozen layer was completely melted away. Based on the observation done in the study, the temperature would give a better indication of the evolution of the frozen bath compared to the voltage drop.

Experiments regarding investigation of the formation of frozen bath underneath newly set anodes were also performed by Picard et al. [23]. The frozen bath samples were investigated using computed tomography and scanning electron spectroscopy (SEM) to qualify the microstructure. To reveal the chemical content of the samples, an energy-dispersive X-ray spectroscope (EDS) was coupled to the SEM. The results from the scanning showed a very different microstructure between the samples. A significantly heterogeneous structure was also found within the same sample. All samples did however have a clear distinction between the alumina phase and the frozen cryolite. In addition, a CT-analysis showed a variety of big pores in the structure. Where they come from is not known, but they are believed to be related to the movement of the gas in the bath.

In a study by Nowicki et al. [24], the opportunities for recovering some of the waste heat found in the primary aluminium industry was investigated to give an overview of the possibilities. The smelters found in Alcoa Deschambault Quebec was used to get this overview. They found that a total of 2 TWh of heat energy were considered as going to thermal waste at the plant. However, only 34 % of this thermal waste were heat which was considered to be easily extractable. Some of the waste heat sources found at the aluminium plant were the exhaust gas from the potlines. Per ton of aluminium produced, the exhaust gas carried out about 3 MWh where the gas had an out temperature of about 100-120 °C. Per year this would account for 770 000 MWh. The surface of the cells was also source of a large thermal waste. Similarly, 3 MWh of waste heat was found per ton of aluminium produced and about 780 000 MWh per year. The accessibility of most of the thermal waste heat sources is however fairly limited due to the complex balance that needs to be maintained inside these pots. In addition, re-building the pots would be a large expense to cover.

Measurements of the temperature and the current pickup of anodes which had been newly set into an electrolysis cell was performed by Ødegård et al. [25]. After 90 minutes of operating inside the cell, no frozen bath could be observed on the side vertical sides of the anode, only on the horizontal side. A substantial temperature reduction was found inside the hot neighbour anodes. This was thought to be caused mainly by the thermal heat radiation from the hot anode to the cold anode. The frozen bath layer would also cause an increased voltage load on the neighbour anodes. Since the frozen layer would have an insulating effect on the current, less current passes through the cold one and thus more must pass through the hotter anodes.

To better understand the impact of the anode change regarding the heat transfer and magnetohydrodynamic flow in the aluminium cells, Wang et al. [26] developed a transient three dimensional coupled mathematical model. Amongst other, they investigated the impact that the temperature on the anodes had on the decrease of temperature on the bath under the newly placed anodes. When the anode was placed in the cell at about room temperature (25 °C), the temperature in the bath decreased from 937 °C to 917 °C 1 hour after the new anodes had been placed in the bath. The temperature of the lower metal was also reduced. The bath under the surrounding new anodes would also gradually solidify as the time progressed. In addition, the velocity decreased from 0.05 m/s to 0.01 m/s. When the temperature of the new anodes was increased from 25 °C to 225 °C, the lowest temperature of the bath increased from 845 °C to 870 °C and the recovery time was reduced from 22.5 to 20 hours.

Chapter 4

Introduction to heat transfer

In the book from Incropera et al., heat transfer is defined as: *Heat transfer (or heat) is thermal energy in transit due to a spatial temperature difference* [27]. Heat transfer will occur whenever there is a temperature difference between media or inside a medium. Heat can be naturally transferred from a media or medium with high temperature to a lower temperature area by three different mechanisms. Conduction occurs if there is a temperature gradient in a stationary medium, which could be either a solid or a fluid. The heat transfer in conduction is caused by collisions between atoms, molecules and/or electrons. Heat transfer through convection will occur between a moving fluid and a surface where there exists a difference in temperature between the two. The last mechanism, thermal radiation, is electromagnetic radiation which comes from the thermal motion of charge particles. Thermal radiation occurs from all surfaces with a nonzero temperature.

4.1 Conduction

The mechanism in conduction is the diffusion of energy due to random molecular motion [27]. In conduction, heat is transferred through direct microscopic collisions between adjacent particles in a medium. When adjacent molecules collide, which is a constant process inside a medium, energy is transferred from the more energetic molecules over to the less energetic molecules. Higher molecular energies will then be associated with higher temperatures [27]. The net transfer of energy through the random collision between particles is often mentioned as a diffusion of energy.

In liquids, the molecules are closer to each other compared to in a gas and the interactions between the molecules are stronger and occurs more often. The

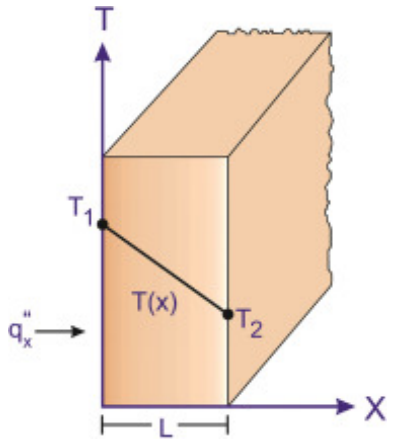

Figure 4.1: The heat transfer of a one-dimensional plane wall by conduction [27]

conduction in a solid due to the vibrations in the lattice. The energy transfer in solids are often described as lattice waves induced by atomic motion [27].

The rate equation for heat conduction is Fourier's law. Rate equations can be used to calculate the amount of energy which is being transferred per unit of time. For a one-dimensional plane, the rate equation for conductive heat transfer is expressed as

$$q_x'' = -k\frac{dT}{dx} \tag{4.1}$$

where the heat flux q_x'' in W/m^2 shows the heat transfer rate per unit area in the x-direction which is perpendicular to the direction of the transfer [27]. This is proportional to the temperature gradient in x-direction. k is the thermal conductivity parameter (W/m $\cdot$ K) and is dependent on the characteristics of the material in which the conduction occurs. The minus sign is used since the heat will be transferred in the direction of the decreasing temperature.

Figure 4.1 shows the heat transfer trough a plane wall under steady-state conditions. The temperature distribution will here be linear. The temperature gradient can then be expressed as

$$\frac{dT}{dx} = \frac{T_2 - T_1}{L} \tag{4.2}$$

and the heat flux accordingly be

$$q_x'' = -k\frac{T_2 - T_1}{L} = -k\frac{\Delta T}{L} \tag{4.3}$$

4.2 Convection

Convection is the transfer of heat due to bulk, or macroscopic, motion of molecules within a fluid such as a gas or a liquid. At any instant, it is assumed that a large amount of molecules are moving as aggregates [27]. The motion of the particles, together with a temperature gradient, will give a heat transfer. Due to the absence of a bulk current flow and no large diffusion of matter, convection won't be able to take place in most of the solids. Convection is however able to take place in some soft solids or mixtures if the solid particles are able to move past each other.

Convection heat transfer is also referred to as the mechanism where heat transfer occur between a solid surface and a fluid in motion when there is a difference in temperature between the two [27].

Convection can be classified as being either natural or forced convection. Natural or free convection occurs due to the buoyancy forces in the fluid. The buoyancy forces are affected by the density differences which are caused by the temperature difference in the fluid. This causes heavier components to fall while lighter components will raise in the fluid. This will result in a bulk movement. Forced convection occurs when an external force such as a fan or a pump is causing the fluid to move. The equation to calculate the heat transfer for convection is expressed as:

$$q = hA(T_s - T_b) \tag{4.4}$$

where h is the convective heat transfer coefficient in $W/m^2 \cdot K$, A is the area given in m^2, T_s is the surface temperature of the solid, and T_b is the average or the bulk temperature of the fluid or gas which is interacting with the surface in K.

4.3 Thermal radiation

Thermal radiation is electromagnetic radiation that is emitted from a material due to the temperature [28]. The radiation is emitted in all directions and will travel at the speed of light directly to the point where it is absorbed. Thermal radiation is emitted by all objects that is at a temperature above absolute zero temperature [27]. As well as thermal radiation emits from solid surfaces, emission will also occur from both gases and liquids. Both the transfer of energy by conduction and convection requires some sort of material medium to occur but the energy transfer using radiation does not. Thermal radiation is in fact most efficiently in a vacuum [27].

The radiation that is emitted by the surface is decided by the thermal energy of the matter that is bounded by the surface. The surface emissive power, E, is the rate at which is energy is released by the surface per unit area (W/m^2) [27].

Equation 4.5 is the Stefan-Boltzmanns law. This equation shows the upper limit to the emissive power, E.

$$E_b = \sigma T_s^4 \tag{4.5}$$

where T_s is the absolute temperature (K) of the surface σ is the Stefan-Boltzmann constant (σ = 5.67 $\cdot$ 10^{-8} W/m^2 $\cdot$ K^4).

The rate of the radiation or the absorption of the thermal radiation from a body is also dependent on the nature of the surface [29]. Surfaces which are good emitters of radiation are also good absorbers. A black surface will be an excellent emitter and absorber while a similar silvered surface will be a poor emitter and absorber [29]. A blackbody is a surface which will absorb all the incoming radiant energy. A blackbody will both be a perfect absorber and a perfect emitter. When calculating the emission power of a perfect emitting surface, such as a blackbody, equation 4.5 can be used. The radiation from a real surface will be less than the radiation a blackbody. The heat flux emitted can be calculated using the following equation

$$E = \varepsilon \sigma T_s^4 \tag{4.6}$$

where ε is the emissivity which is a radiative property of the surface. The emissivity has a value within the range $0 \leq \varepsilon \leq 1$. This value shows how will the real surface emits energy when compared to a blackbody. Most materials have an emissivity of about 0.7. Polished materials will have a low emissivity at about 0.1.

In addition to the thermal radiation that emits from a surface, the radiation could also be incident on a given surface from the surroundings. This could e.g. be radiation from the sun on the planet or from a bonfire to the surrounding people. The irradiation, G, will be the rate of all of the incident radiation on a unit area of the surface, regardless of the source [27].

As mentioned previous, the amount of absorbed radiation is dependent on the nature of the surface. The amount of absorbed energy will affect how much the thermal energy of the material is increased. The rate of absorbed radiant energy per unit surface energy on a real surface is dependent on the absorptivity, α, of the material. That is,

$$G_{abs} = \alpha G \tag{4.7}$$

where α is the absorptivity coefficient. The absorptivity coefficient has a value within the range $0 \leq \alpha \leq 1$. If $\alpha < 1$ and the surface is opaque, some of the irradiation hitting the surface will be reflected of the surface. A part of the irradiation might also be transmitted through the material is the surface is semi-transparent. The sum of these three effects will decide the absoptivity coefficient [28].

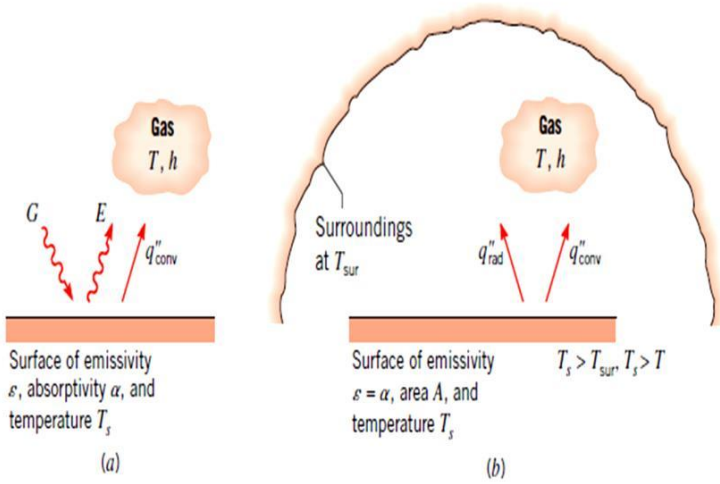

Figure 4.2: The exchange of radiation (a) at a surface and (b) between a surface and large surroundings [27].

$$\alpha = 1 - \rho - \tau \tag{4.8}$$

where ρ is the reflection factor and τ is the transmission factor. The value of α does also depend on the nature of the irradiation. The absorptivity of a solar radiation might be different compared to the radiation from a furnace [27].

When the radiation occurs between a small surface which has a temperature T_s and a much larger isothermal surface that is surrounding the smaller surface, such as in Figure 4.2 (b), the heat exchange can be calculated using Equation 4.9 [27]. The surrounding surface could for example be the walls of a room. If one assumes that there is a grey surface ($\alpha = \varepsilon$), one can express the rate of radiation heat transfer from the surface as

$$q_{rad} = \frac{q}{A} = \varepsilon E_b(T_s) - \alpha G = \varepsilon\sigma(T_s^4 - T_{sur}^4) \tag{4.9}$$

Chapter 5

Experimental work

The experiments were performed at Alcoa's aluminium plant in Mosjøen, Norway. All the experiments of the current pick-up rate were performed on the same aluminium cell and following one anode change schedule. The investigation of the formation of frozen bath underneath newly set anodes and measurements inside the cell were performed on different cells.

5.1 Setup

Figure 5.1: A photograph of one of the two anode containers which were used to pre-heat the carbon anodes. The anode container has been insulated in the bottom to reduce the heat loss to the ambient air outside the container. The bottom was insulated with a layer of heat resistant plates and then a layer of barrier bricks. During experiments, the space between the side walls and the anodes and butts as well as the top was insulated with Rockwool and insulating blankets.

The pre-heating process was performed in the standard anode containers used in Alcoa Mosjøen. The anode containers were insulated using a layer of heat resistant plates in the bottom followed by a layer of barrier bricks, as shown in Figure 5.1. The cold anode was then placed in the centre of the insulated anode container with 4 standard K-type thermocouples placed into each anode. During the experiments, one butt was placed on each side of the cold anode inside the insulated anode container. The temperature data from the thermocouples were stored on a potable logging unit (AAC-2, INTAB, Sweden). A total of 4 butts were then used to pre-heat the 2 anodes at each experiment. During the pre-heating process, the top of the anode and the butts were covered in mineral wool from Rockwool and insulation blankets. The walls of the anode container were also insulated with the same insulation as the top. The anodes were then heated for 1, 2, or 4 hours in this system and then placed into the aluminium cell as a part of the standard anode change. The positions of the thermocouples inside the anodes can be found in Figure 5.2. A drilling machine was used to drill the holes in the anodes to place the thermocouples. The thermocouples were drilled 30 cm straight down into the anode. The anodes have a height of about 60 cm, so the thermocouples would measure the temperature at about midway.

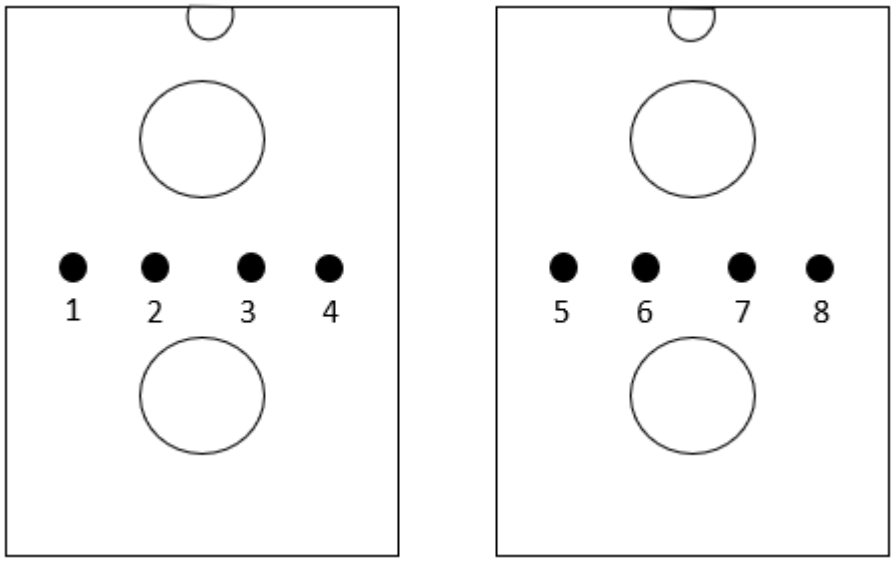

Figure 5.2: A sketch of the position of the thermocouples inside the cold anodes. The holes where the thermocouples were placed into were drilled 30 cm straight down into the anode. The anodes themselves are about 60 cm high, so the thermocouples measures the temperature close to the middle.

An aluminium cell was chosen by the engineers to perform the experiments on. This particular cell was chosen since it was a stable cell. A logger was mounted on the aluminium cell which continuously monitored the voltage drop. The voltage drop is measured over a specific length between the crossbeam and the current supply bar. The signals are then amplified. Since the voltage drop will be monitored over the same length at all the anodes and the material remains the same, the voltage drop is only dependent on the current. The measurements could however be affected to some extend by the temperature. When a new anode is placed into the cell it will have a larger resistance compared to the anodes which has been operating for a couple of days and has reached their desired operating temperature. A larger resistance in an anode will result in less current passing through that anode and accordingly less voltage drop. A lower resistance in the anode will cause a larger voltage drop. The measurements are not precisely calibrated, but they are mostly used for an error diagnosis. The logger can therefore not be used to calculate the local current consumption for each anode, but more to observe the fluctuation of current to each anode. The voltage values presented in the graphs from the logger will therefore not show the actual consumption, but compared to data taken from previous anode settings the values can be used to view the impact from pre-heating the carbon anodes and if there is a difference in the amount of current passing through the anodes when they are pre-heated.

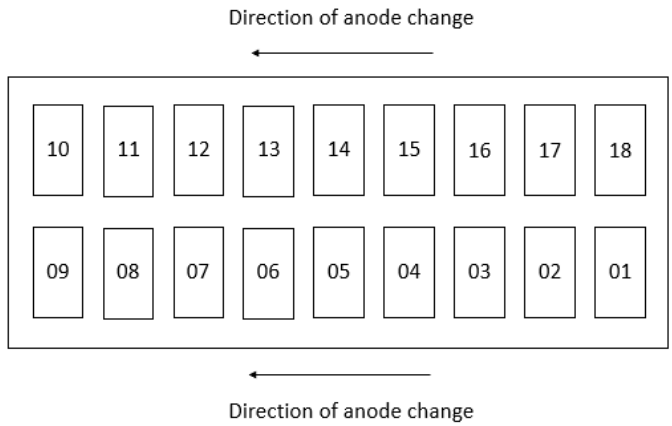

Figure 5.3: The figure shows an illustration of the positions of the anodes in the aluminium cell used to performed the experiments. The anodes were changed in pairs. First anode 01 and 02 were changed, then 03 and 04, and so on till anode 09 which is changed separately. Then anode 18 is also changed separately, before anode 17 and 16 is changed in pairs all the way over till anode 10 and 11. Between the change of two anodes, or one for anode 09 and 18, there will be 2 or 3 days. After about 1 month all the anodes have been changed once.

Figure 5.3 shows the positions of the anodes inside the aluminium electrolysis cell. To make it easier to distinguish the different anodes when referring to them later in the thesis, each anode is given a number in the cell which follows the anode change schedule. The anode change schedule is explained in Figure 5.3. All the anodes used in these experiments were changed in pairs and the outermost anodes were not used. An anode change activity is performed every 2 or 3 day at an aluminium cell where either a pair of anodes are changed or just a single one is changed if it is anode 09 or 18. After about 1 month, all of the anodes in the cell has been changed and the anode change cycle will start from the beginning again. This is a continuous cycle and will continue as long as the cell is operating. Each anode therefore has a life cycle of about 1 month.

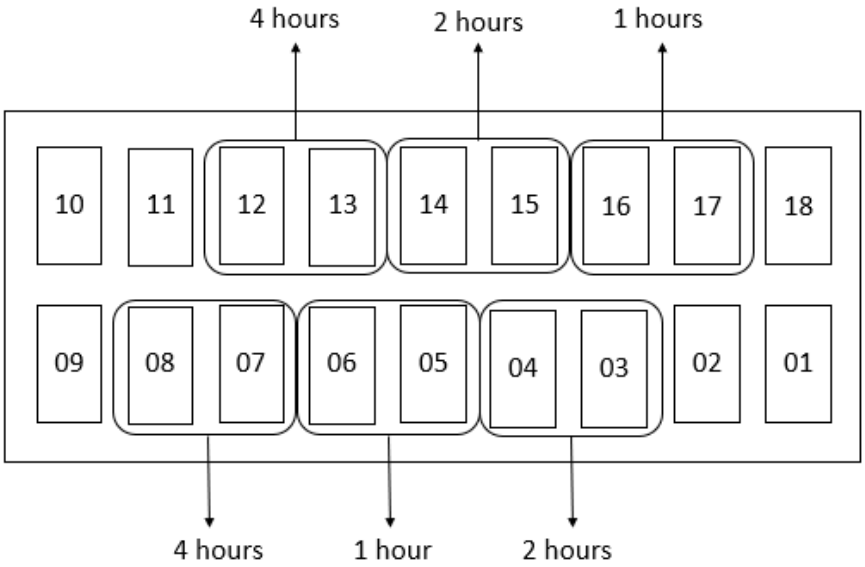

Figure 5.4: The figure is similar to Figure 5.3. This figure shows the number of hours the anode pair had been pre-heated within the anode container before it was placed into the cell and where they were placed.

Figure 5.4 shows the position of the pre-heated anodes inside the cell. The number of hours in the figure shows for how long the anode pair had been pre-heated before they were placed into the cell. Since the experiments follows the anode change schedule it took a bit less than 1 month to perform all the experiments with the pre-heated anodes.

5.1.1 Computed tomography

Cone beam computed tomography, CBCT, uses an imaging technique where a x-ray source and a detector have a fixed rotation around an object or the object itself is rotating. The x-ray source will emit a cone-shaped source of ionising radiation which will pass through the object which is of interest. This rays will be detected by the x-ray detector on the opposite side [30]. A sketch of the principle is seen in Figure 5.5. Then there are two different methods used. Either the object will be in a fixed position and the x-ray source and detector will rotate around the object or the source and the detector will be in a fixed position and the object will rotate. The machine used to perform these experiments used the principles of the rotating object. The object is then rotated around its own axis for 360 degrees while several images is being taken [31].

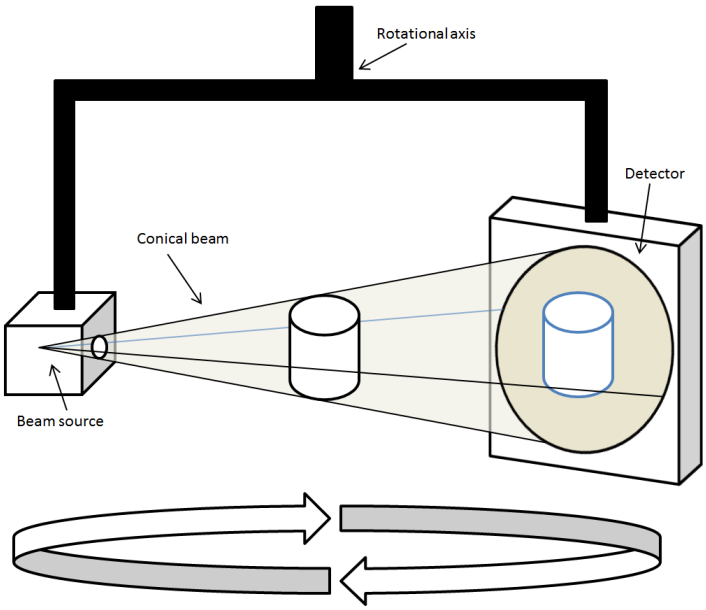

Figure 5.5: The figure shows the principle of cone beam computed tomography [32]. The x-ray source emits a cone-shaped x-ray source which passes through the selected sample and is detected by an x-ray detector on the opposite side. Then, either the sample or the source and the detector is rotated 360 °while pictures are taken. This figure shows the variant where the sample is in a fixed point and the x-ray source and detector moves around the sample.

To increase the resolution of the images, half of the samples needed to be reduced in size. This was done by using a large table saw and cutting the samples into smaller bits.

5.1.2 Values in cell

Figure 5.6 shows the position of where the measurements were taken at three different heights in the cell. The measurements were taken on three different height to give an average value of the air velocity and temperature between the anodes. The measurements were performed in multiple cells to assure that the values did not only matter for one cell. The environment in the cells did vary to some extent. Depending on the age of the anodes where the measurements takes place, temperature in the bath, amount of crust, distance to the feeding holes, cell performance etc. the values will vary.

To do the measurements of the air velocity, a pitot tube was connected to a TSI 9565 velocicalc multi-functional ventilation meter. The pitot tube would measure the off-gas sucked in by the fume collector placed in the hood inside of the aluminium cell. The measurements were performed by sticking in the pitot tube in between the side covers of the cell. This was done as opposed to removing one of the covers as this would increase the air flow into the cell. When the pitot tube where placed in the right location the measurements started on the ventilation meter. The device logged the air velocity for 10 seconds and calculated the average value over the 10 seconds. When the measurements where done in one spot, for example spot 1 in Figure 5.6, it was moved up to spot 2 and the same procedure was done. When all three measurements were done, a new position between two cells where chosen in the same cell or in a new cell.

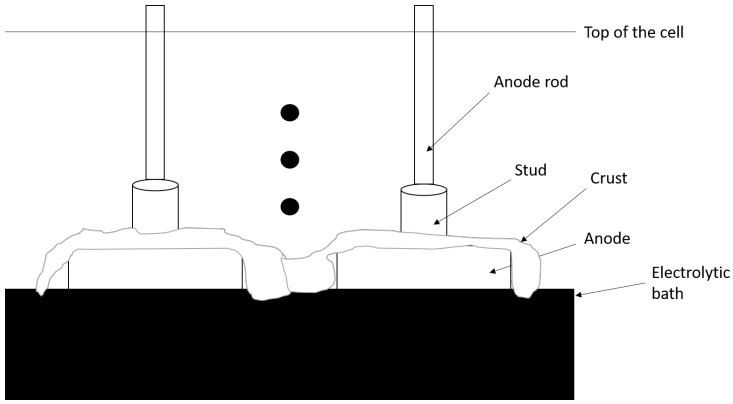

Figure 5.6: An illustration of where the air velocity and the temperature values were measured. The three dots show approximate position in the cells between the anodes where the measurements were performed. While Figure 2.1 shows the cross section from the short side this figure shows the cross section from the long side. The values were measured between different anodes in multiple cells.

These measurements were performed to look at the possibility of pre-heating inside the aluminium cell using the heat of the air inside the cell and the radiating heat from the electrolytic bath and the anodes. The present work will however mainly focus on the pre-heating using the butts from the process. This is because pre-heating inside the cell would most likely result in a large expense because the cell would have to be redesigned to fit an anode inside the cell above the bath.

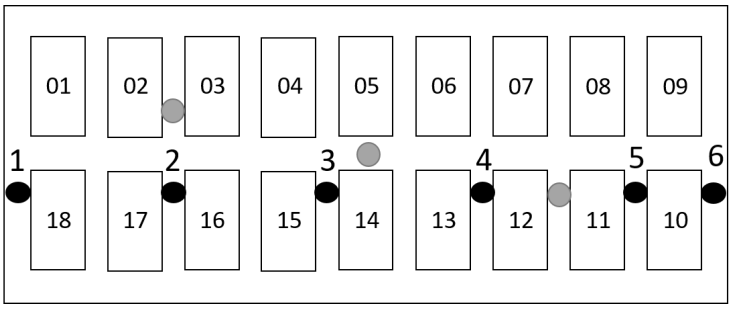

Figure 5.7: The black dots shows the position where the different measurements took place inside the cell. The grey dots show the position of the point feeders in the cells. Here there will be an opening down to the bath. The positions are used in Table 6.2.

5.1.3 IR-camera

The thermal images were taken with a FLIR T440 thermal imaging camera. The camera was used to picture the surface temperature on the side walls and underneath for 2 pre-heated anodes and 2 butts using infrared light. The use of an IR-camera will give a broader visualisation of the temperature distribution across the anode compared to the thermocouples which would only measure the temperature in one point. The IR-camera would however only be able to measure the surface temperature of the anode. The surface temperature underneath the anode and the centre temperature could give important information of how well the temperature is distributed. The IR-pictures of the side walls of anodes were taken when the anode was being lifted up from the anode container. The pictures from the bottom surface were taken seconds later when the anodes were transported to the aluminium cells where they were going to be placed into the electrolytic bath. The IR-pictures of the butts were taken after the butts were removed from the cell and during the transportation over to the anode containers.

5.2 Matlab

The description for the functions used in Matlab is described in the documentation for Matlab version R2019a. To make the current pick-up data more readable and easier to interpret, a curve fitting function was used to construct a continuous curve or mathematical function to best fit the supplied data [33]. The current data collected from the logger would be fairly fluctuating, so a 5th degree polynomial of the values was created to improve the readability. In Matlab, the function polyfit uses the supplied data points and the degree of the polynomial that will give the best fit for the data (in a least-squares sense). Here, p will be the coefficients in descending powers and the length of p will be n+1.

$$p(x) = p_1 x^n + p_2 x^{n-1} + ... + p_n x + p_{n+1} \tag{5.1}$$

The function polyfit will also return a structure S that can be used to calculate the error estimates for each point using the function polyval. The function outputs an estimate of the standard error in predicting a future observation at x by p(x).

5.3 Statistics

5.3.1 Probability distribution

The most important continuous probability distribution within statistics is the normal distribution [34]. The normal distribution was developed by Carl Friedrich Gauss and is used to describe the distribution of measurement errors [35]. The normal distribution is a often a good model at predicting the distribution of variables that is representing many natural phenomena which may be fairly symmetrical, such as rainfall studies and measurements of manufactured parts [35]. An illustration of the normal distribution is presented in Figure 5.8. The horizontal axis in the figure represents all of the specific values x that the random variable X presents, and the vertical axis shows the density for each x values [36]. The normal distribution is continuous for all values of X and therefore has a theoretically range which includes all real numbers. This means that every real number has a nonzero probability and the curve will only approach the horizontal axis but never touch it. Since the normal distribution is continuous, the probability density is shown by the height of the curve. The area under the curve between two coordinates of x is equal to the probability that the value of the random variable X is between the two x-coordinates. The area under the whole curve is 1.00.

The normal density function follows the following mathematical equation:

$$f(x; \mu, \sigma^2) = \frac{1}{\sqrt{2\pi\sigma^2}} e^{-\frac{1}{2\sigma^2}(x-\mu)^2}, -\infty < x < \infty \tag{5.2}$$

where μ is the mean of the distribution, σ^2 is the variance, and σ is the standard deviation [34]. μ can be any finite number, while σ^2 has to be a positive finite number [36]. The standard deviation is the square root of the variance for a distribution. It is a measurement which can be used to quantify how much variation there is in for a set of data values [37].

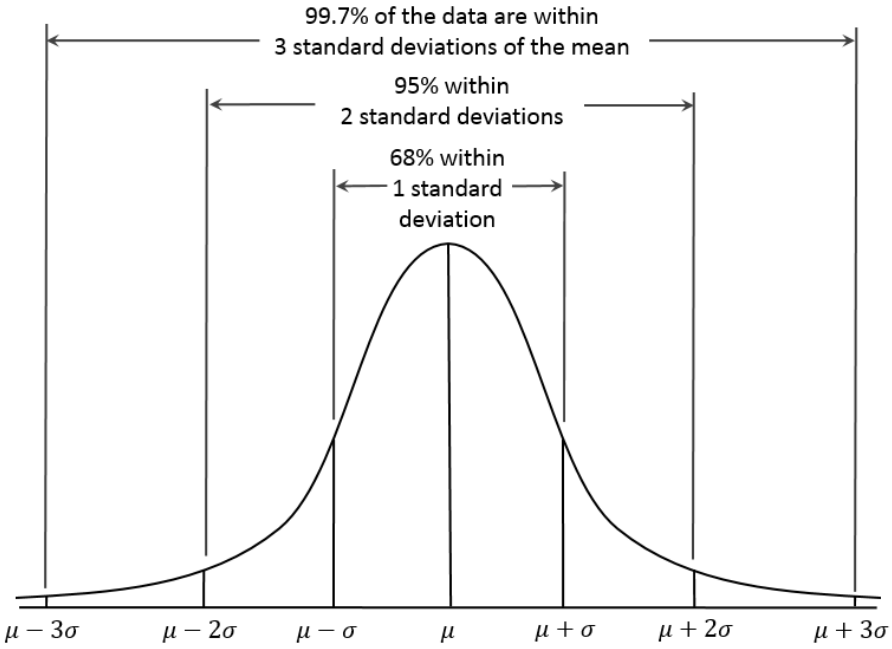

Figure 5.8: A sketch of the probability density function for normal distribution. The figure shows that one standard deviation away from the mean will contain 68.27 % of the values, two standard deviations away from the mean is 95.45 % and three deviations is 99.73 % [38].

5.3.2 Student-t

$$T = \frac{\bar{X} - \mu}{S/\sqrt{n}} \tag{5.3}$$

The Student t-distribution, or just t-distribution, is another continuous probability distribution. $\bar{X}$ is the mean of the sample, S is here the estimator for population standard deviation, and n is the degrees of freedom. The shape of the student-t probability density function is also quite similar to the normal distribution. However, when applying the normal distribution, it is assumed that the standard deviation is known. In experimental scenarios where the standard deviation is unknown and the sample size is small, the probability distribution will differ significantly

from the normal distribution. For large numbers of degrees of freedom, n, where degrees of freedom is one less than the number of observations, the probabilities in the Student t-distribution will approach the normal probabilities [36]. The Student t-distribution can then be used if it's known that the distribution is Gaussian and the σ is unknown, because the t-distribution will take into account the spread of the σ's. Since the true value of the standard deviation is unknown, the standard error shown in Equation 5.4 is the standard deviation of the t-distribution.

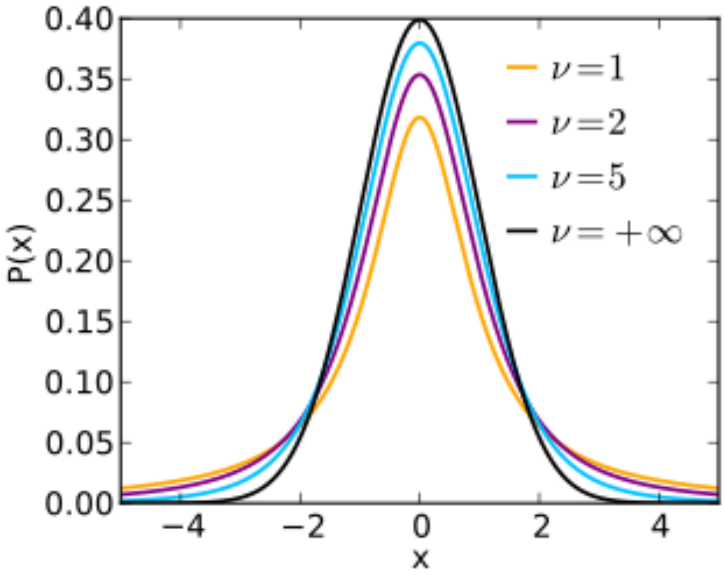

Figure 5.9: A sketch of the probability density function for student-t distribution. The figure shows how the function approaches the normal distribution as the degrees of freedom approaches infinity [39].

$$\sigma_M = \frac{\sigma}{\sqrt{N}} \tag{5.4}$$

The standard error (SE) is the standard deviation of the sampling distribution of a statistic [40]. When a sampling distribution of a population mean is acquired, the distribution of the different means will have its own variance and mean. The variance, which shows the degree of spread, of this distribution will then be variance of the population divided by the size of the sample. When the number of samples gets larger, the means of the samples will tend to form around the mean of the population. An increase in sample size will lead to a reduced variance of the sampling distribution. As shown in Equation 5.4, the standard error is equal to the standard deviation divided by the square root of the sample size.

Chapter 6

Results

This chapter will present the results obtained for this master thesis. Temperature values from the pre-heating process using both thermocouples and infrared camera, logging device to monitor the voltage drop over the anodes, and samples from the frozen bath which will form underneath newly set anodes.

6.1 Temperature

This section will present the temperature data received from the thermocouples placed in the carbon anodes to measure the temperature during the pre-heating section. An illustration of the position of the thermocouples inside the carbon anodes is shown in Figure 5.2.

Figure 6.1 shows the average temperature for the centre positions inside the carbon anodes for 1 hour, 2 hours, and 4 hours of pre-heating. The temperature values for position 2, 3, 6, and 7 were used to find the average temperature value in the middle of the anode. The temperature values were not able to be collected from all the experiments, but a total of 14 temperature measurements were used to calculate the average temperature values for pre-heating 1 hour, 10 temperature measurements for 2 hours, and 6 temperature measurements for 4 hours. One temperature measure can be from either one of the four positions in the middle part, position 2, 3, 6 or 7. In addition, the first hour of pre-heating for 2 hours and 4 hours were added to the temperature measurements for pre-heating 1 hour and the first 2 hours of pre-heating for 4 hours were added to the temperature measurements for 2 hours. This was done since the pre-heating method remained the same and to increase the amount of temperature measurements.

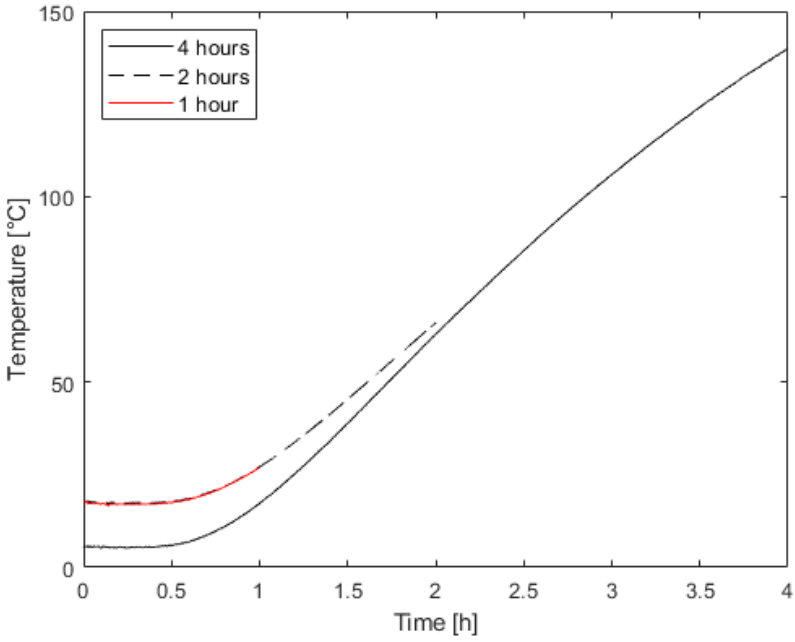

Figure 6.1: The figure shows the average temperature in the middle positions 2, 3, 6, and 7, as shown in Figure 5.2, as a function of the time spent pre-heating with the butts inside the insulated anode container. One temperature measurement is from either one of the middle positions.

Figure 6.1 shows that the temperature close to the centre of the carbon anode on average is 26.9 °C for 1 hours of pre-heating, 66.1 °C for 2 hours, and 140.0 °C for 4 hours.

An attempt to measure the temperature of the butts whilst inside the anode container was also performed. This was done by placing one thermocouple against the wall of the remaining carbon block of the butts. This will of course measure the surface temperature of the butt and not the core temperature. A fairly large temperature difference can be seen between the two butts in Figure 6.2, and this is probably due to the placing of the thermocouples. This was just done to gain an estimate of the surface temperature of the butts and how much energy is possible to extract from the butts, and for how long it is useful to perform the pre-heating using butts.

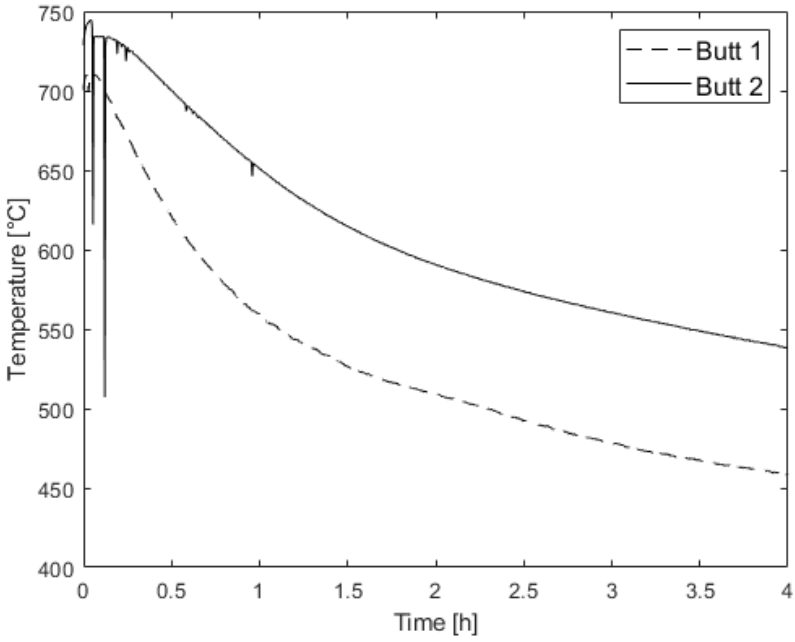

Figure 6.2: The temperature profile of the two butts used to pre-heat anode 12. The temperature was measured by placing one thermocouple against the remaining part of the butt as well as possible.

Figure 6.3 shows the average temperature for the side positions inside the carbon anodes for 1 hour, 2 hours, and 4 hours of pre-heating. The temperature values for position 1, 4, 5, and 8 were used to find the average temperature value in the side of the anode. The positions are illustrated in Figure 5.2. It was not possible to obtain a full set of temperatures from all the experiments, but a total of 12 temperature measurements were used to calculate the average temperature values for pre-heating 1 hour, 10 temperature measurements for 2 hours, and 6 temperature measurements for 4 hours. Similar to the measurement of the average temperature in the middle positions in Figure 6.1, the measured temperatures for 4 hours were also used in the temperature values for 1 hour and 2 hours.

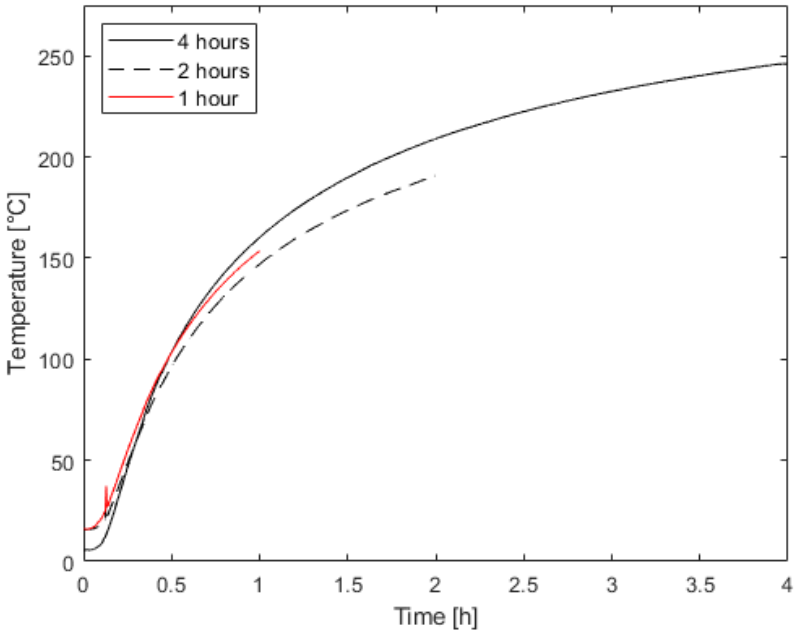

Figure 6.3: The figure shows the average temperature in the side positions 1, 4, 5, and 8 as shown in Figure 5.2 as a function of the time spent pre-heating with the butts inside the insulated anode container. One temperature measurement is from either one of the side positions.

Figure 6.3 shows that the temperature on the sides of the carbon anode on average is 153.4 °C for 1 hours of pre-heating, 190.6 °C for 2 hours, and 246.1 °C for 4 hours.

6.2 Energy saving

Table 6.1: Parameters and values used to calculate the energy saving from pre-heating carbon anodes.

Parameters	Value
Mass of anode, [kg]	1300*
Mass of butts, [kg]	325*
Molar mass carbon, [g/mol]	12.01
Molar mass aluminium, [g/mol]	26.98
Core temperature in anode before heating, [°C]	5
Core temperature in anode after heating, [°C]	140
Molar heat capacity carbon, J/(K · mol)	10.202**
Anode life cycle, [s]	2 592 000
Line current, [A]	175 000
Number of anodes in cell	18
Faraday's constant, C/mol	96485

* = This is an estimation of the weight of the anodes and the butts used

** = An average value of the heat capacity between 273.15 K and 450 K [41]

When a new anode is placed into the electrolytic bath in an aluminium cell in connection with the anode change process, the whole anode must be heated up to an operating temperature where the anode is at its highest temperature. This operating temperature is assumed to be close to the bath temperature. Consequently, the anode must be heated up from about 5 °C and up to a temperature which is close to the bath temperature. This energy must be taken from the electrolytic bath. Figure 6.1 shows the average temperature in the core of the pre-heated carbon anodes after 1, 2, and 4 hours. These temperature values are here assumed to be the average temperature in the anode and will be used in the following calculations. The amount of energy that has been given to the carbon anode by pre-heating using butts can be found by using the following equation for heat:

$$Q = n \cdot c_p \cdot dT \tag{6.1}$$

where Q is the heat, n is the mole, c_p is the molar heat capacity, and dT is the temperature difference. By applying the law in Equation 6.1 it's possible to give a estimate of how much energy is given to the carbon anode from the two butts inside the insulated anode container. The physical values are given in Table 6.1. Pre-heating the carbon anode from 5 °C to 140 °C results in 149.1 MJ of energy

supplied to the anode from the two butts. 149.1 MJ will be the theoretical amount of energy that is saved from pre-heating the carbon anode, so when the pre-heated anode is placed into the electrolytic bath its average temperature will be 140 °C and it needs less heat compared to a non pre-heated anode placed into the bath with an average temperature of 5 °C. By dividing the amount of energy saved on 3600, which is the quantity of seconds in one hour, 41 kWh of energy is saved from the pre-heating.

The theoretical production of electrode product formed can then be calculated by applying Faraday's law of electrolysis, Equation 2.7. This gives a theoretical mass of 2348.9 kg aluminium produced per anode over its whole life cycle using a 100 % current efficiency.

Dividing the quantity of energy saved on the amount of aluminium produced over the life cycle of the anode, the result is 0.018 kWh/kg Al. Per kilogram of aluminium produced it is then possible to save 0.018 kWh worth of energy.

6.3 IR-images

An infrared radiation (IR) camera was used to visualise the temperature distribution in the carbon anode in a different way compared to the thermocouples. The IR-camera creates a heat zone image of the surface where the camera is pointed towards, also called a thermogram. The camera was used to visualise the temperature after the pre-heating of anode 5 and anode 7 which were pre-heated for 1 and 4 hours respectively, as well as the temperature of two butts which were used to pre-heat anode 5 and 6.

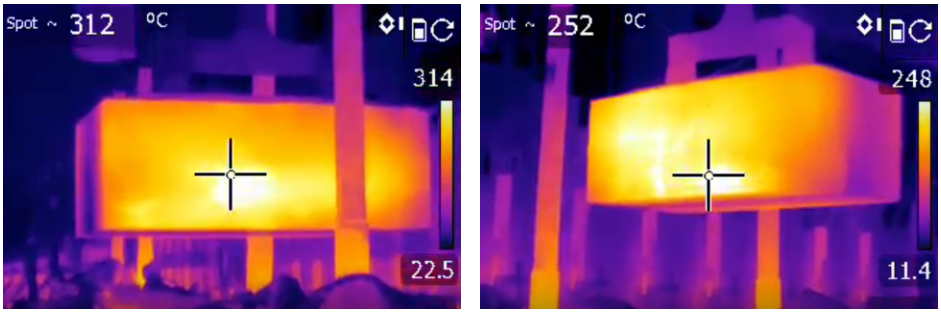

(a) Anode 5 pre-heated for 1 hour **(b)** Anode 7 pre-heated for 4 hours

Figure 6.4: The two images shows the surface temperature on one of the side walls of pre-heated anode 5 and 7 using an IR-camera. Anode 5 has been heated for 1 hour and anode 7 has been heated for 4 hours. In the image they were being lifted out of the anode container where the pre-heating took place. Since the butt only has about one fourth of the height of an anode, the highest temperature is typically a bit below the middle of the side wall. The temperature shown in the top left corner of the images is the temperature within the middle of the plus sign. The bar on the right shows the heat of the different colours. This is the surface temperature measured right after the anode is removed, the surface temperature will decrease over time when exposed to the surrounding air.

Figure 6.4a shows an IR-image of one of the side walls of the anode which has been heated for 1 hour. From the image, one can see that the highest temperature measured on the side wall which were closest to the butt and exposed to the most radiation reached a surface temperature of 312 °C. The thermocouples measuring the temperature on the same side as the image in position 1 and 2, from Figure 5.2, measured a temperature of 169.8 °C in position 1 and 98.0 °C in position 2. The image presented in Figure 6.4b shows the surface temperature of anode 7 when it has been lifted from the anode container. Here, the surface temperature was measured to be 252 °C. The measured temperature in position 1 were 250.2 °C and 148.8 °C in position 2.

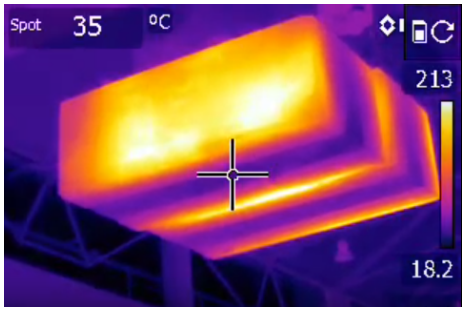

(a) Anode 5 pre-heated for 1 hour

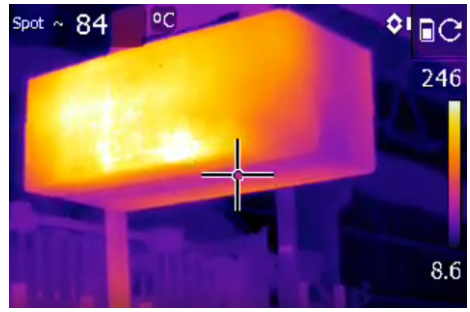

(b) Anode 7 pre-heated for 4 hours

Figure 6.5: The image shows the surface temperature on the bottom of anode 5 and 7 which has been pre-heated for 1 hour and 4 hours respectively. For anode 5 there is a clear difference in colour on the bottom and the side part on the anode is due to the slots in the anode. They cause a layer of air between inside the anode which reduced the heat flow in the bottom of the anode. For anode 7 the difference in temperature is less and the heat has been able to spread more inside the anode.

The same anodes as in Figure 6.4 was also photographed from the bottom to see how the temperature had been distributed throughout the anode. This will show a bit more of the total effect the pre-heating will have. After 1 hour of pre-heating the anode will have a fairly high temperature on the side wall, but the heat would not have had enough time to spread inside the whole anode as can be seen in Figure 6.5a. After 4 hours the heat has been able to penetrate more into the centre. The bottom of the anode in Figure 6.5b has a temperature which is twice as big as in Figure 6.5a. The surface temperature of the sides are however larger after 1 hour, but this has to be due to the temperature of the butts decreasing over time, as can be seen in Figure 6.2.

(a) Side of butts

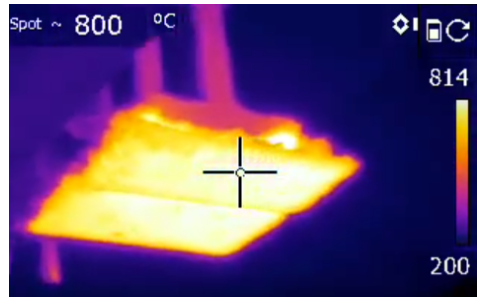

(b) Bottom of butts

Figure 6.6: The image shows the surface temperature on the butts as they are removed from the cell and being transported to the anode containers.

Figure 6.6 shows two IR-pictures taken of the butts as they are removed from the cell and being transported over to the anode container.

6.4 Current pick-up

This section presents the voltage drop for the anodes to give a presentation of the difference in amount of current passing through and out to each anode, which is explain more thorough in the Experimental chapter. As mentioned previously, the anodes were changed in pairs and both anodes were pre-heated. The anodes in the outermost positions, position 1, 2, 9, 10, 11, and 18, were not used. The pre-heated pair of anodes were then compared to anodes that has been changed previously in the time period from December 2018 to February 2019. The position of the anodes inside the cell can be found in Figure 5.3. An illustration of where the different pre-heated anodes were placed is shown in Figure 5.4. The standard error of the measurements is added to the plots as dashed lines. The error bounds will correspond to approximately 95 % confidence interval.

Since the position of the anodes in the cell are believed to have a large impact on the process, the graphs have been organised by their position in the cell. The positions in the cell can be found in Figure 5.3. The positions are of such importance due to the curvature of the metal caused by the magnetic field. The metal bath decides the interpolar distance, the distance between the anode and the cathode. The aluminium cells used to perform the experiments in this work are organised in an end-to-end configuration. This configuration, compared to the side-to-side configuration, often causes high magnetic field values, especially as the current in the cells has increased over the years to increase the production capacity and reduce the operating costs [1]. The current will cause a magnetic field which will result in the metal to be highest underneath the middle anodes and be lower towards the ends.

To give clearer presentation of the voltage drop data, a polynomial curve fitting was used on the data. The voltage data will have a continuously fluctuation due to the electrolytic bath always being in movement and the temperature fluctuation. The standard error bounds were added to the plots to investigate if there is a statistical significance in the measurements. The voltage drop data for the pre-heated anodes were compared to voltage drop data for normal anodes which had been set previously, anodes that has not been pre-heated. The positions of the pre-heated anodes correspond to the position of the normal anodes for each graph. Since the anodes in Alcoa Mosjøen are changed in pairs, the average voltage drop value for the pairs has used. As an example, for Figure 6.7a the ”pre-heated”-line shows the average voltage drop for the pre-heated anode 3 and 4, and the ”normal”-line shows the average voltage drop value for two anodes which has been set in position

3 and two anode in position 4, so the average voltage drop for a total of 4 anodes.

The first set of anodes presented is the pairs 3 and 4, and 12. An error had occurred so the measurements for anode 13 had not been logged. Anode 3 and 4 were pre-heated for 2 hours while anode 12 were pre-heated for 4 hours. Their position in the cell will be similar but on the opposite side of the cell. They will both have two anodes on their right side and the rest of the anodes on their left side. Figure 6.7 shows the voltage drop across the pre-heated anodes and the values from normal anodes in their respective positions.

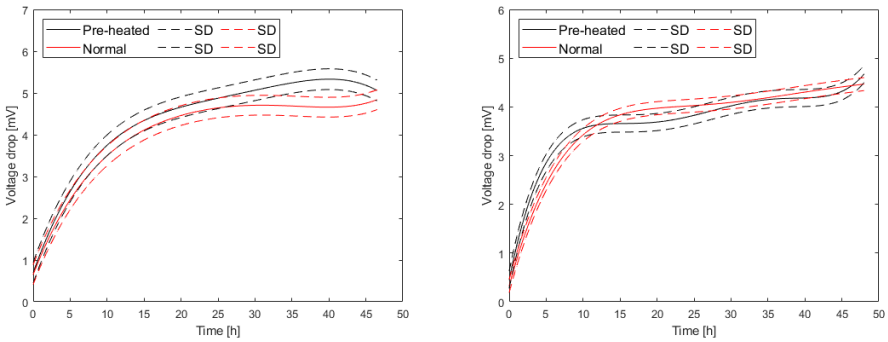

(a) Anode 3 and 4, pre-heated for 2 hours **(b)** Anode 12, pre-heated for 4 hours

Figure 6.7: The figures shows the voltage drop across the anodes for the selected positions. Anode 3 and 4 has been pre-heated for 2 hours while anode 12 has been pre-heated for 4 hours. These positions will be the same in the cell on each side of the electrolysis cell. The voltage drops across the newly set pre-heated anodes were compared to measured voltage drops across previous set anodes. The voltage drop for 4 normal anodes in the same positions were used for both anode 3 and 4, and anode 12 and 13. The standard error for the measurements corresponding to about 95 % confidence interval were also added to the lines.

The next positions are those which are most centred in the cell. Figure 6.8 shows the voltage drop across both the pre-heated anodes and the normal anodes from previous anode changes. Figure 6.8a has an x-axis which only goes to 18 hours due to the measurements of the pre-heated anodes were disconnected at this point.

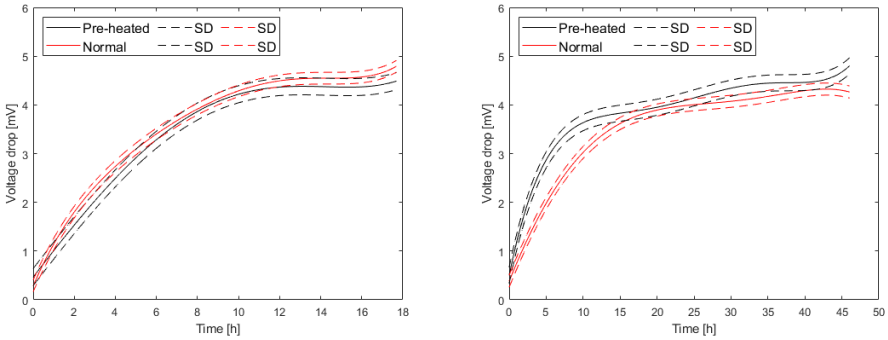

(a) Anode 5 and 6, pre-heated for 1 hour **(b)** Anode 14 and 15, pre-heated for 2 hours

Figure 6.8: The figures shows the voltage drop across anode 5 and 6 which has been pre-heated for 1 hour and anode 14 and 15 which has been pre-heated for 2 hours. Values from 4 anodes were used to create the normal line for position 5 and 6, and 4 anodes were used for position 14 and 15.

The last positions of the outermost pairs that were measured is found in Figure 6.9. 4 anodes were used on each pair to create the values for the normal anodes.

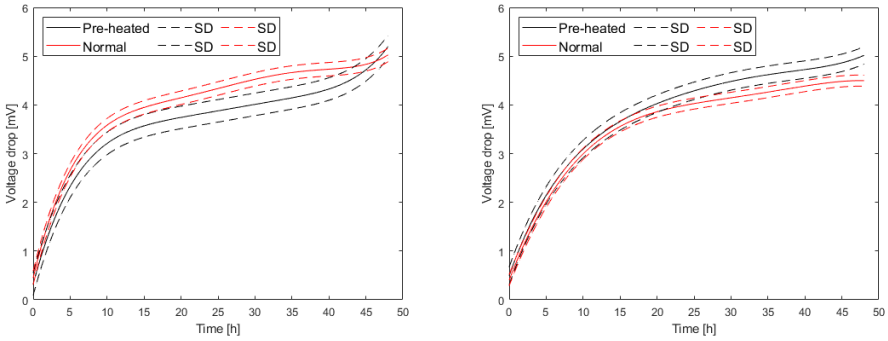

(a) Anode 7 and 8, pre-heated for 4 hours **(b)** Anode 16 and 17, pre-heated for 1 hour

Figure 6.9: The figures shows the voltage drop across anode 7 and 8 which has been pre-heated for 4 hour and anode 16 and 17 which has been pre-heated for 1 hour. Values from 4 anodes were used to create the normal line for position 7 and 8, and 4 anodes were used for position 16 and 17.

6.5 Investigation of frozen bath

An investigation of the formation of frozen bath underneath pre-heated anodes compared to underneath normal anodes were also performed. This was done by pre-heating one anode and not pre-heating the other one. Since the anodes are changed in pairs in Mosjøen one will be able to see the difference in frozen bath underneath the pre-heated one and the non pre-heated one. Three different pre-heating time periods of 1 hour, 2 hours, and 4 hours were decided to be used. Due to some problems with the crane that changes the carbon anodes the anode which was pre-heated for 4 hours couldn't be removed from the cell and one were unable to investigate the frozen bath layer underneath this anode. So a total of 3 experiments were performed to investigate the frozen bath layer but only the anodes which were pre-heated for 1 hour and 2 hours were able to be removed from the cell to be investigated.

The experiments were done by pre-heating one anode inside the same insulated anode containers using butts as previously for the other pre-heating experiments. The anodes were pre-heated for the desired time period. Since the anodes in Mosjøen are changed in pairs, the pre-heated anode and a non pre-heated anode was placed into a chosen cell at the same time. After 4 hours inside the cell they were both removed. Samples were then taken of the frozen bath for further investigation using computed tomography (CT) machine.

Figure 6.10 and 6.11 shows the frozen layer of the pre-heated anode and the normal anode when they have been removed from the cell. A large portion of the frozen bath did fall of in the process of removing the anodes from the bath. This was the frozen bath between the two anodes. When the anodes were taken out of the cell they are able to move slightly independently of each other due to how the crane works, so this probably made it so some of the layer fell off. So the areas between the two anodes where there is a mark from the frozen bath, it probably was removed when the anodes were taken out of the cells. The removed frozen bath samples can be seen in Figure 6.12 and 6.13.

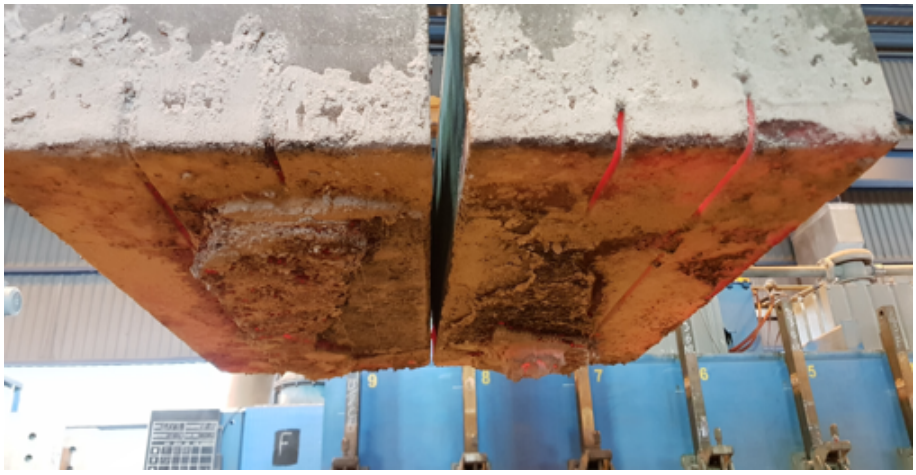

Figure 6.10: The formation of the frozen bath underneath two anodes is showed here. The anode to the right was pre-heated for 1 hour using butts inside an insulated anode container. Then the pre-heated anode and a regular non pre-heated anode, the one to the left, was placed into an aluminium cell for 4 hours. The pre-heated anode was placed in position 7 and the non pre-heated one in position 8. Both anodes were then removed from the cell and samples were collected.

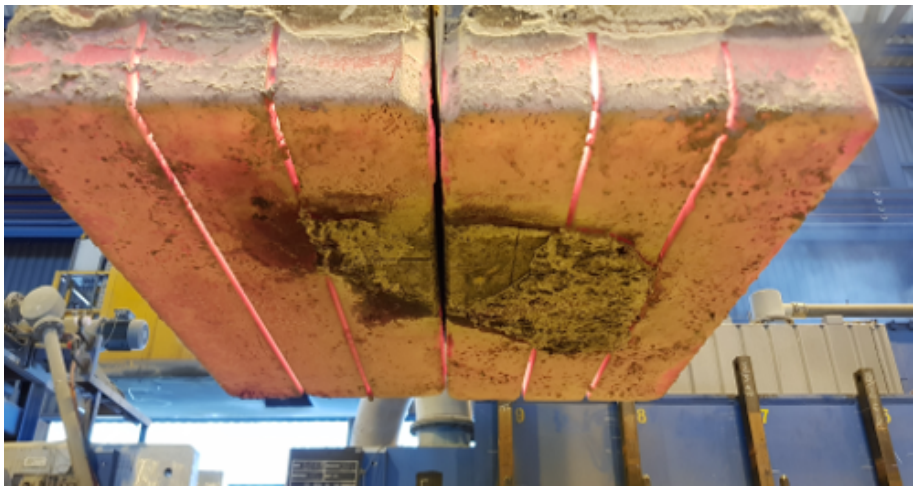

Figure 6.11: The formation of the frozen bath underneath two anodes is showed here. The anode to the left was pre-heated for 2 hours using butts inside an insulated anode container. Then the pre-heated anode and a regular non pre-heated anode, the one to the right, was placed into an aluminium cell for 4 hours in position. The pre-heated anode was placed in position 12 and the non pre-heated one in position 13. Both anodes were then removed from the cell and samples were collected.

(a) Anode 7 Back

(b) Anode 8 Back

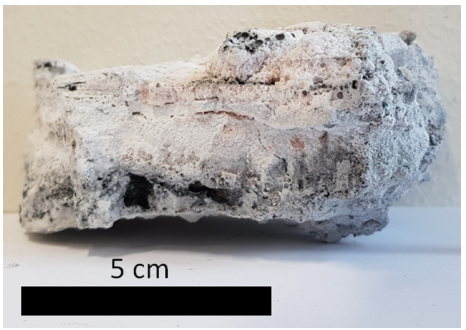

(c) Anode 7 Middle

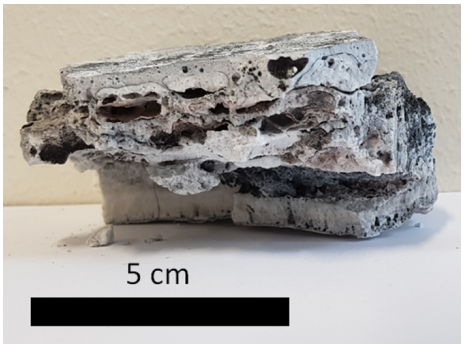

(d) Anode 8 Middle

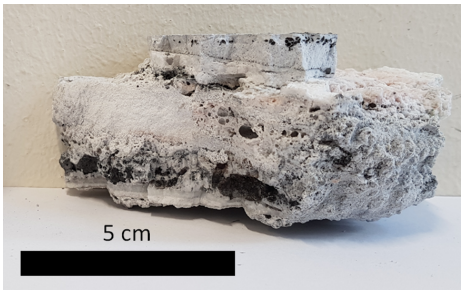

(e) Anode 7 Front

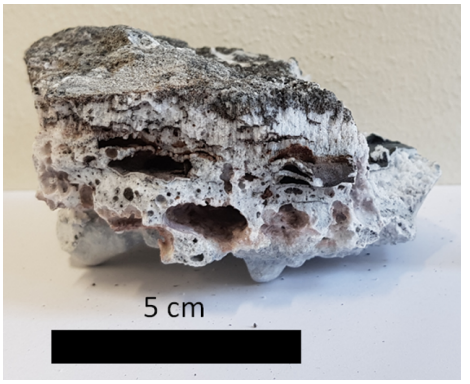

(f) Anode 8 Front

Figure 6.12: Frozen bath samples from anode 7 and 8. All the samples except Figure 6.12a and 6.12e are orientated so the surface on top was the surface in contact with the anode and the bottom was in contact with the bath.

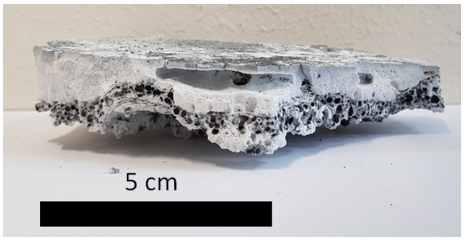

(a) Anode 13 Back

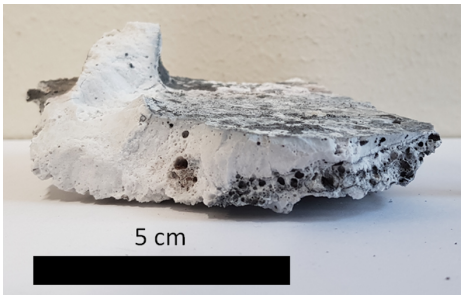

(b) Anode 13 Middle

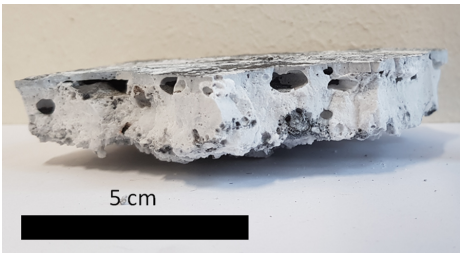

(c) Anode 13 Front

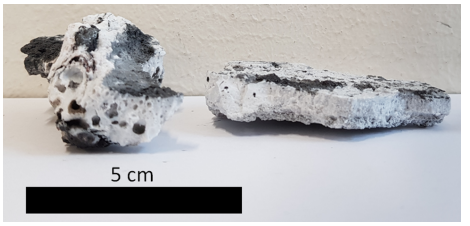

(d) Anode 12

Figure 6.13: Frozen bath samples from anode 12 and 13. All the samples are orientated so the surface on top was the surface in contact with the anode and the bottom was in contact with the bath.

Figure 6.12 shows the frozen bath samples from anode 7 and 8. Here, anode 7 was pre-heated for 1 hour while anode 8 was not pre-heated. Both anodes were placed into the cell for 4 hours before they were removed and the frozen bath samples were collected. Figure 6.13 shows the frozen bath samples from anode 12 and 13. Anode 12 were pre-heated for 2 hours while anode 13 were not pre-heated.

The samples collected from the back can be seen as the part which is furthest away from the camera in Figure 6.10 and 6.11. This is also the position which was furthest into the cell. The front is closest to the camera and is closest to the opening.

6.6 Computed tomography

An analysis of the samples from the formation of the frozen bath underneath the carbon anodes were performed using a computation tomography (CT) machine. The frozen bath was removed from the underside of the anodes after the anodes were removed from the cell. A total of 10 samples of frozen bath were gathered. 3 samples were collected from anode 7, 8, and 13 while only 1 sample were collected from anode 12 since there was so little frozen bath underneath it. On the anodes where 3 samples were collected, it was attempted to collect samples at different positions under the anode. One sample from the spot which is closest to the side covers of the cell, one in the middle of the underside and one which is closest to the centre.

Due to the limiting space in the chamber of the CT-machine and the resolution of the machine, some of the larger samples had to be cut into smaller parts to be able to receive a better image from the CT-machine. The pictures showing the frozen bath samples have the top part of the samples is what were in contact with the anode and the bottom part is the part that were in contact with the bath. This applies for all of the pictures in Figure 6.12 and 6.13 except for Figure 6.12a and 6.12e which are opposite.

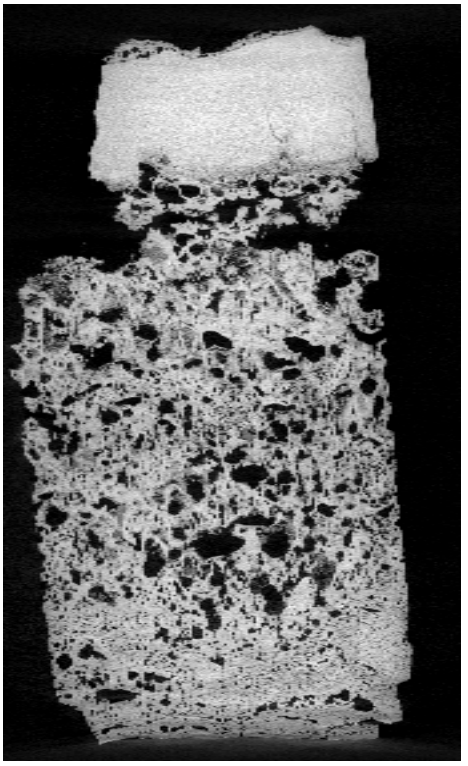

(a) Anode 7 Back

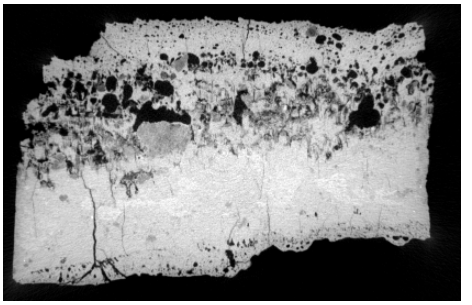

(b) Anode 8 Back

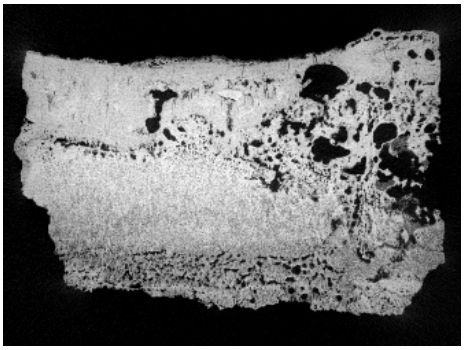

(c) Anode 7 Middle

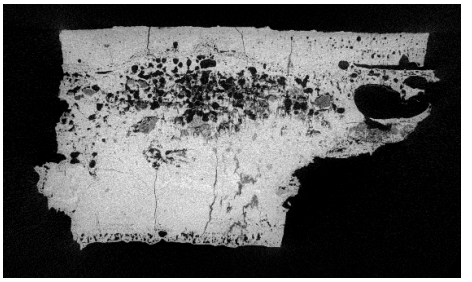

(d) Anode 8 Middle

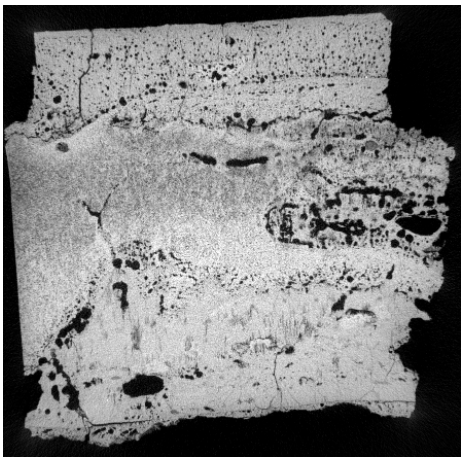

(e) Anode 7 Front

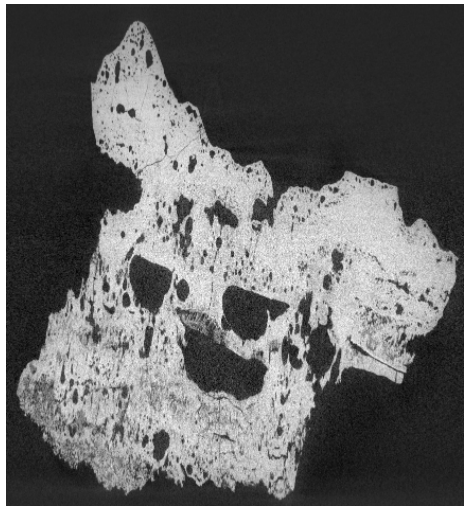

(f) Anode 8 Front

Figure 6.14: CT-scan of frozen bath samples from anode 7 and 8. The images are oriented as in Figure 6.12.

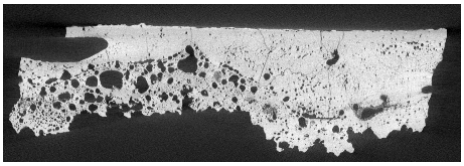

(a) Anode 13 Back

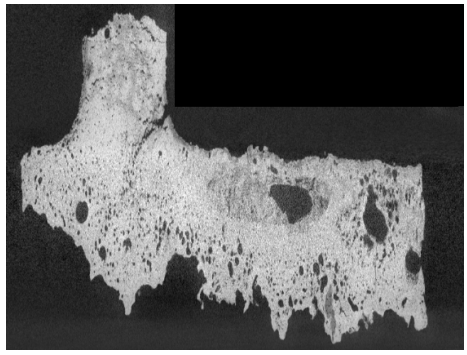

(b) Anode 13 Middle

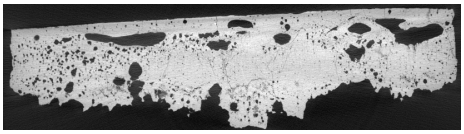

(c) Anode 13 Front

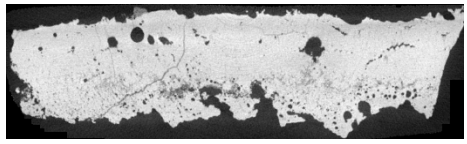

(d) Anode 12

Figure 6.15: CT-scan of frozen bath samples from anode 12 and 13. The images are oriented as in Figure 6.13.

6.7 Values inside the cell

The values that were measured inside the cell were put into Table 6.2. The values were measured as described in the Experimental setup. A total of 5 aluminium cells were used to collect the information about the velocity and the temperature inside the cell. The position in cell where the information was collected is found in Figure 5.7. Not every position in each cell was used as a measuring point.

The velocity and temperature was measured in three different heights in each position, as shown in Figure 5.6. The average value of these three points were then put into Table 6.2. The same was done for the temperature values. These were measured in the same positions and then calculated the average value. In addition, the age of the neighbour anodes of the measurements were added. The measurements were performed between the anodes, except for the corner anodes, so the table shows the age of the anode on the left and on the right.

Table 6.2: The table shows the air velocity and temperature values measured using a pitot tube and a thermocouple. Since the measurements were performed between the anodes, except for the corner anodes which only has one anode, the age of the neighbour anodes is added. The column shows the age of the left and right anode in days since they were placed into the bath. The position in the cell is shown in Figure 5.7.

Position in cell	Average Velocity [m/s]	Average Temperature [°C]	Age of neighbouring anodes in days
4	1.22	130.5	8 - 8
4	1.24	148.2	2 - 2
3	1.34	-	20 - 20
2	0.84	143.8	7 - 7
6	0.94	135.4	7 -
1	1.19	151.8	- 18
6	1.38	-	3 -
5	1.03	152.0	3 - 3
2	1.21	154.7	6 - 3
4	1.10	141.9	6 - 6
3	1.03	164.5	9 - 9
1	1.24	140.1	- 21
5	1.26	161.5	21 - 21
2	1.12	-	19 - 19
4	0.91	-	16 - 16
3	0.94	-	16 - 16

The total average value for the air velocity inside the cell were 1.12 m/s. The average value for all the temperature measurements were 147.7 °C.

Chapter 7

Discussion

7.1 Temperature

Temperature data presented in the Results section proved that the temperature increased inside the carbon anodes using butts as a heat provider. According to the heating experiments, the centre positions of the anode reached about an average temperature of 140 °C after being heated for 4 hours. It did however take about 30 minutes before the heat reaches the thermocouples which are were in the centre of the anode. Looking at Figure 6.1 one can see that after the 30 minutes mark the temperature will start to raise and after about 1 hour the temperature will continue to raise at a constant pace. Even after 4 hours of pre-heating the temperature will continue to increase in the centre. Looking at the figure which shows the average temperature values for the side positions, Figure 6.3, one can see that the temperature starts to increase rapidly very quickly after the butts has been placed by the side of the anode. The temperature in the side positions will however start to decline at an earlier rate than in the centre positions. This will naturally occur as the temperature of the butts decreases. The average temperature of the butts in Figure 6.2 shows how the temperature decreases over time. After the 4 hours, the butts have decreased from above 700 °C to about 500 °C in this particular measurement of the surface temperature of the butts. The temperature for the butts were measured at the surface of the block.

By looking at the temperature in the centre of the anodes after the specific time periods, it shows that pre-heating for just 1 hour won't give a significant increase of temperature in the anode. Since it takes about 30 minutes before the temperature starts to raise in the centre this is half of the heating time. Since in the end the whole anode must be heated up to an operating temperature inside the cell, a high temperature in the centre of the cell would be beneficial. Analysing

the temperature graphs shows that the temperature in the centre will continue to raise even after 4 hours. The temperature in the side positions however won't increase much more after 4 hours. Since the temperature in the side positions looks like it is about to reach its max temperature at about 250 °C, no more energy will be transferred from the butts to the anode as the temperature of the butts also will continue to decrease. This could imply that after 4 hours of utilising the heat from the butts there won't be that much more energy to take advantage of. The centre temperature could still raise some more but since the side temperature won't increase much further, there won't be any new energy added to the anode. This is based on the heating procedure performed for these experiments. There are different factors that could have been optimised to further improve the heating process, such as the distance between the anode and the butts, insulation of the container, and transportation between the heating station and electrolysis cell.

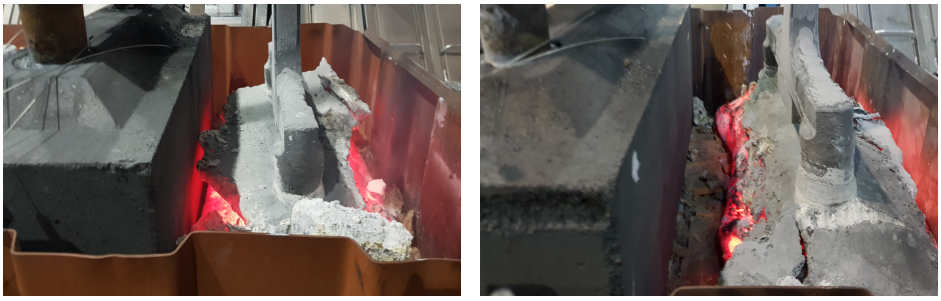

(a) A short distance between the anode and the butt

(b) A large distance between the anode and the butt

Figure 7.1: The images shows the difference between a short and a large distance between the anode and the butts. This would affect the amount of heat transferred. A larger distance would create an insulating layer of air between the anode and the butts which will reduce the heat transfer.

Figure 7.1 shows an example of a short and large distance between the anode and the butt. The temperature measurements of the anode which had a large distance were used to investigate how the temperature is affected by the difference in distance between the anode and the butts. The impact of the distance between the anode and the butts can be seen in Figure 7.2 and 7.3 which shows the average temperature in the side position and the centre position compared to the temperature measured in a side of an anode where the distance between the anode and the butt where fairly large.

As mentioned in the Experimental section, the distance between the anodes and the butts inside the anode container during the pre-heating could vary between touching each other and up to 15 cm apart. The distance between the anode and the butts is believed to have an impact on the heat transfer. To visualise how the distance affected the temperature and heat transfer, the temperature measurements of a case where the distance was about 15 cm was compared to the average temperature measurements. Both the side temperature and the centre temperature are shown in the following figures. The anode used to illustrate this difference is one of the sides used when investigating the amount of frozen bath. An example of the impact that the distance between the anode and the butts has on the side temperature is shown in Figure 7.2.

Here, the anode was heated for 2 hours. If the heating process would last for 4 hours one would probably see a larger difference in temperature. After 2 hours of heating the anode with the long distance is about 50 °C lower on the side and about 20 °C in the centre. The start temperature is however about 10 °C lower for the long distance anode probably due to the cold ambient temperature in the pot room. In this case, the distance between the anode and the butt was roughly 15 cm. The larger layer of air between the anode and the butt will reduce the heat transfer since air is not a particularly good substance to use for heating. Since the butts have a temperature of above 700 °C in the beginning and 500 °C towards the end after 4 hours, it is assumed that the heat radiation will affect the heating process the most. A larger distance between the two objects will of course reduce the thermal radiation received by the anode. Other factors could also affect the case in Figure 7.2 and 7.3 such as the mass of the butts, time before the butts and anodes were covered, and transportation time from the cell to the anode container, but it is reasonable to assume that the distance between the anode and the butts could greatly affect the amount of heat transferred over time.

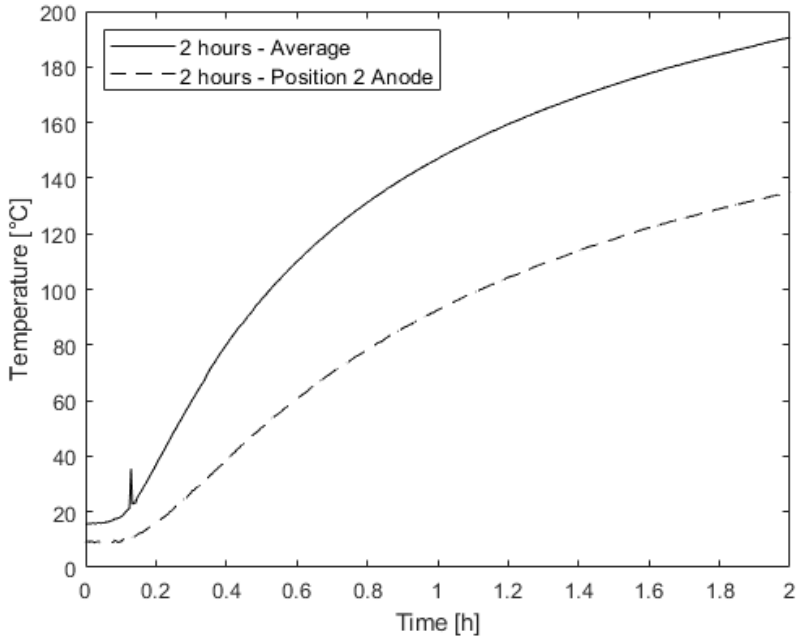

Figure 7.2: The figure shows an example of the distance between the anode and the butts could affect the temperature distribution in the anode. This is probably the incident where the distance between anode and butt were the largest. The distance between the anode and the butts were approximately 15 cm at the maximal. The average temperature line is from Figure 6.3 and shows the temperature values for the positions 1, 4, 5, and 8 which are the outermost positions

The same anode was used to see the temperature difference in the centre position. Figure 7.3 shows the temperature the next position, compared to the average centre temperature. This figure will show how the distance affects the temperature in the centre.

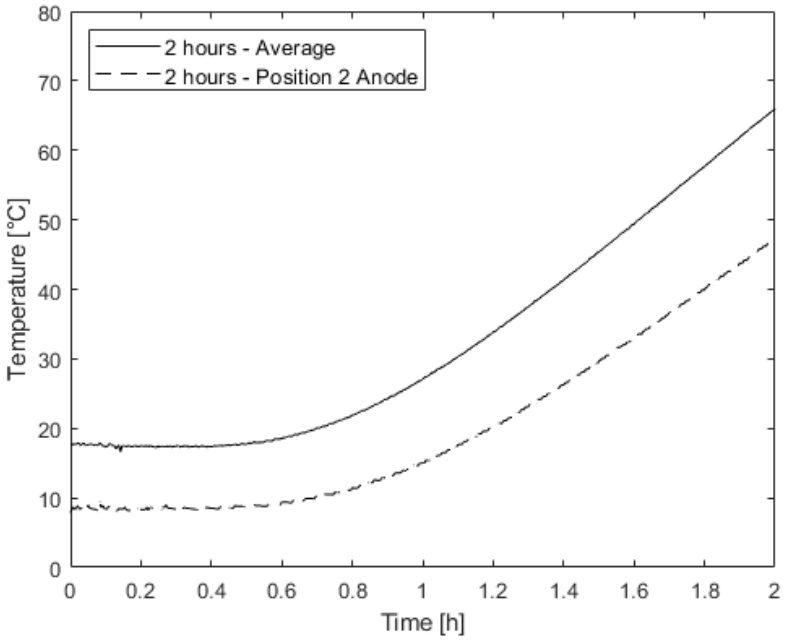

Figure 7.3: The figure shows the temperature in position 2 of the same anode presented in Figure 7.2. Position 2 is mostly dependent on the heat from position 1, but heat from position 3 and 4 will of course affect the temperature in position 2. The average temperature line is from Figure 6.1 and shows the temperature values for the positions 2, 3, 6, and 7 which are the positions close to the centre.

From the figures one can observe that the distance between the anode and the butts will have an effect on the temperature inside the anode. A larger distance between the anode and the butt will result in a lower temperature inside the anode due to the loss of heat caused by the larger air space between. The temperature difference is more prominent in the outer positions in the anode (Position 1, 4, 5, and 8) rather than the positions near the centre of the anode (Position 2, 3, 6, and 7).

7.2 Energy saving

The calculation of the possible energy saving from the pre-heating turned out to be 0.018 kWh/kg Al. These are of course only theoretical values but gives an estimate of how much it is possible to save by pre-heating the anode. The value was calculated from the amount of energy saved by pre-heating it up to 140 °C as this would reduce the amount of energy needed to be taken from the bath. Since

the anode would have to reach an operating temperature close to the temperature of the bath to function normally, this pre-heated temperature would give a head start. The benefits of for instance reduced disturbance to the cell or increased current pick-up rate is not included in the calculations.

It is assumed here that the anode reaches a temperature of 140 °C over the whole anode. Since we only know the temperature at 4 spots inside the cell and the surface temperature using the IR-camera, it was assumed that the temperature measured close to the centre of anode gave a reliable average value. The temperature at the bottom centre surface showed to be less than 140 °C, but the temperature at the side surfaces showed to be much larger than 140 °C. If one assumes that Norway produces 1.2 million tonnes of aluminium a year and every carbon anode was pre-heated to the temperature of 140 °C so 0.018 kWh/kg Al was saved, this would turn out to be 21.6 GWh energy saved a year for the production in Norway. For the whole production of aluminium in the world, 64.3 million tonnes, this would be 1.16 TWh energy saved a year. Optimising the pre-heating station with for example better insulation or reducing the distance between cell and station would also improve the energy savings.

7.3 Current pick-up

The voltage plots were presented in a sequence depending on their position in the cell as opposed to the amount of time they were pre-heated for. This was done because it is believed that the position in the cell would greatly affect the current pick-up rate of the anode due to the temperature profile of the cell and the curvature of the liquid metal. The magnetic field created by the flow of electric current will affect the liquid metal bath and create a curvature on the metal. The liquid metal will have the highest point in the middle and lower towards the ends of the cell. So the voltage plots were presented as the pairs who have the similar positions in the cell on the opposite sides.

In the plots, a polynomial fitting was used on the data plots of the voltage drop to give a best fit of the data. A polynomial degree of 5 was found to be the most fitting for the data points. A confidence level of 95 % was added to the observed data to show the confidence of that the parameter will lie within the interval. This confidence level was added to both the observed data for the pre-heated anodes and the normal anodes. The confidence intervals can also be used to determine if the results are statistically significant different.

The two first anode pairs which were presented were placed in position 3, 4, 12, and 13. The average values for the pre-heated anodes in this position showed a little larger voltage drop compared to the average values of the normal anodes in the initial 12 hours of operating in the cell. A larger voltage drop would be due to a

lower resistance across the anode. The pre-heating process is assumed to be most beneficial in between the initial 24 hours. After the first 24 hours it is assumed that the both the pre-heated and the normal anodes will approach their operating temperature and then the pre-heating wouldn't give any further advantages. In the initial 24 hours it has been proved that the pre-heated anodes will have an increased current pick-up rate compared to a non pre-heated anodes, as mentioned in the Literature review. This was of course with temperatures much higher than obtained in this study. In this case, the benefit of the pre-heating is marginal by just looking at the voltage drop. The voltage drop is of course dependent on several conditions than just the temperature of the anode.

There is however little to no statistically significant difference between the pre-heated anodes and the normal anodes for the two pairs in this position. For there to be a significant difference between the results the standard deviation lines must not overlap. If the two dashed lines which shows the standard deviation at a 95 % confidence level does not overlap, there is a 95 % confidence that the two results do not overlap and that the pre-heating would have a benefit when considering the voltage drop.

The next two pairs were found in position 5, 6, 14, and 15. These positions were the most centre positions in the aluminium cell. Position 5 and 14 would be the middle position in the cell. These positions give fairly different results. Anode 5 and 6 which were pre-heated for 1 hour showed no benefit from it. The voltage drop of the pre-heated anodes were in fact a bit underneath the voltage drop for the normal anode pair the whole time. Anode 14 and 15 which were pre-heated for 2 hours showed a large benefit from the pre-heating process. In the plot one can see that there is a statistically significant difference between the pre-heated anodes and the normal anodes in the initial 12 hours. After the initial 12 hours, the average voltage drop for the pre-heated anodes continued to stay above the normal anodes.

The last anode pairs are the positions of 7, 8, 16, and 17. Here one sees that the voltage drop for the pre-heated anode 7 and 8 lies significantly underneath the voltage drop for the normal anodes. One would assume that the longer pre-heating would have a larger benefit to the voltage drop but there might be other processes that affect the voltage drop more such as the interpolar distance or operation conditions like the bath temperature or bath composition. The last pair, anode 16 and 17, showed a small benefit of the pre-heating but the with a overlap of the confidence interval.

In total for these measurements one can't say that the measurements are statistically significant different since the standard deviation lines overlapped for most of the graphs. If the dashed lines did not overlap one could say that with a 95 % confidence there is a significant difference. Even though some of the pre-heated anodes showed a large difference between the lines, such as anode 14 and 15, this

was not the case for all the other pre-heated anodes. One would assume that the longer the anodes are pre-heated the faster they will be operating in the cell. According to the graphs, the anodes pre-heated for 2 hours showed the best results while anode 7 and 8 which were pre-heated for 4 hours showed the lest benefit. The pre-heating process has been proven to be beneficial in previous studies, but in these case, there might be other steps in the process that affect the voltage drop across the anodes more.

To draw a conclusion whether the pre-heating has a benefit on the amount of current passing through the anode, more experiments would have to be performed. For most of the graphs, the average value of two pre-heated anodes were compared to the average value of four normal anodes. This means that if for example one anode or one of the pairs were placed a bit too high above the metal this would greatly affect the graphs. The anodes in Mosjøen were placed into the bath manually so to hit the exact mark could be fairly difficult to do with the naked eye, so a few millimetres difference from the mark is to be expected. If one assumes that a 1 cm above the mark is a worst-case scenario, as seen in the calculations this could case up to a 0.3 mV difference in the graphs. If the normal anodes were placed only 5 mm under the mark and one pre-heated anode 5 mm above the mark this could greatly affect the plots. The curvature of the metal bath would also then have an impact on the resistance in the bath. This would most likely affect the outer positions the most. This could also cause an uneven flow of current through the anode since the interpolar distance would be shorter on one of the sides compared to the other side. Since there also only was time to perform 1 pre-heated anode and 2 normal anodes in each position, one deviation could greatly affect the results. One would need more experiments to be able to exclude these deviations and to have a more reliable result.

Even though the current pick-up rates did not show any statistically significant difference would all logic suggest that pre-heating would benefit the process. It would benefit by reducing the disturbance to the cell since the anodes already have a higher temperature and would need less time to reach an operating temperature compared to a normal cold anode. However, it is difficult to estimate how much these benefits would mean for the current pick-up rate.

7.4 Calculation of interpolar distance

As mentioned previously, the distance between the anode and the cathode, the interpolar distance, will have a significant impact on the resistance in the bath. The voltage drop across the electrolyte accounts for about 1.7 V. Increasing the interpolar distance will result in a larger voltage drop. To give a rough estimate of how much an additional 1 cm has on the voltage drop across the bath, a calculation

of this was performed. Here, the calculations were performed by measuring the voltage drop across the anode rod while the measurement done by the logger used to perform the current pick-up plots measured the voltage drop across a material before it reaches the anode rod, as mention in the experimental setup. The principles are however the same and this would give a similar estimate of error as the standard deviation. The calculations cannot be used directly on the voltage plots presented in the Results section but more of an estimate of how 1 cm can affect the plots.

Table 7.1: The table shows the values used to calculate the increase in voltage drop as the interpolar distance is increased in an aluminium cell.

Parameters	Value
Total current, [kA]	175*
Cell voltage, [V]	4.5*
Areal of surface under carbon anode, [cm^2]	8250
Cross-section of material for voltage drop, [cm^2]	10
Electrical conductivity cryolite, [S/cm]	3.0
Electrical conductivity aluminium, [S/cm]	377 000
Length of measured voltage drop material, [cm]	15

* = This is an estimation of the current and cell voltage

The anodes in the aluminium cell is connected in a parallel circuit. Calculating the total resistance in the cell under normal operation can be found by applying Ohms law when the total current and cell voltage is known. Here we assume that the resistance across all the anodes is the same. By changing the distance between the anode and the cathode, the interpolar distance, the anode will experience an additional resistance. The voltage drop across the electrolyte account for a large part of the resistance in the cell and it is proportional to the interpolar distance.

The tool used to measure the current out to the anodes for this experiment would measure the voltage drop. The voltage drop is measured over a short distance across the anode rod. Following equations can be used to calculate the voltage drop

$$\Delta U' = \frac{dx}{\kappa_{Al} \cdot A} \cdot I_i \tag{7.1}$$

where dx is the length of the measurement of the voltage drop, A is the cross-section of the measured material, κ is the electrical conductivity of the conducting material, and I is the current to anode i. The anode rod is here made of aluminium.

The resistance in the material is multiplied with the current passing through resulting in the voltage drop across the two measure points. Since the resistance in the material is assumed to be constant, the voltage drop will be proportional to the current.

Assuming that the resistances in each anode are the same under normal operation, the resistance to each anode will be

$$\frac{1}{R_{tot}} = \sum_{i=1}^{n} = \frac{n}{R} \Rightarrow R_{tot} = \frac{R}{n} \tag{7.2}$$

If the interpolar distance is changed, this will affect the resistance. An increased interpolar distance will make a larger resistance while a decreased distance will reduce the resistance. The resistance to anode i adjusting for the change in interpolar distance will be

$$\tilde{R}_i = R + \frac{\Delta ACD}{\kappa_{bath} \cdot A_{anode}} \tag{7.3}$$

where R is the resistance in the anode at normal operation, Δ ACD is the change in interpolar distance, κ is the electrical conductivity of the electrolytic bath, and A_{anode} is the surface area of the bottom of the anode.

By using Ohms law it is then possible to calculate the amount of current passing through an anode which has had a change in its interpolar distance. $\tilde{U}_c$ is the voltage out to the anode. In a parallel circuit the voltage will be the same for all the connections. We assume that the interpolar distance will not affect the total cell voltage. The local resistance to the specific anode which was had its interpolar distance changed will experience a different resistance, as shown in Equation 7.3. Then it is possible to calculate the new current out to the anode.

$$\tilde{I}_i = \frac{\tilde{U}_c}{\tilde{R}_i} = \frac{T_{tot} \cdot R_{tot}}{n \cdot R_{tot} + \frac{\Delta ACD}{\kappa_{bath} \cdot A_{anode}}} = \frac{\Delta U_c}{n \cdot \frac{\Delta U_c}{I_{tot}} + \frac{\Delta ACD}{\kappa_{bath} \cdot A_{anode}}} \tag{7.4}$$

When the anode is at normal operating conditions the current to each anode will be 9722.2 A. If an anode is placed 1 cm above the normal interpolar distance, the current will be 8941.7 A. So, a 1 cm difference in interpolar distance can greatly affect the process. In addition, the other anodes in the cell will experience a larger current due to the less current passing through the anode placed too high. If the anodes are changed in pairs and both are placed too high, this will affect the cell even more.

Equation 7.1 can then be used to calculate the new voltage drop across the anode rod with the new current. This is the same measure point as used in the figures in the Results section. If one assumes that 1 cm over average interpolar

distance is the maximum height the anode can be placed in by inaccuracy, this can cause an increase of 0.31 mV on the measurement. The interpolar distance is however difficult to measure since the metal always has some sort of movement.

These calculations focused only on the difference in voltage drop across the anode rod when one anode is placed at a higher interpolar distance. The other resistances were assumed to be constant. A higher interpolar distance could however affect the cell in other ways. The anode could experience a lower local temperature since it is placed higher in the bath. Since the higher anode also has a higher resistance there will be a larger current load on the neighbouring anodes.

7.5 Investigation of frozen layer

The formation of frozen bath underneath normal and pre-heated anodes after a given time were investigated. From the images of the frozen bath underneath the anodes one can see a clear difference between the pre-heated anode and the non pre-heated anode in both cases. For anode pair 1, where one anode was pre-heated for 1 hour, the layer underneath the non pre-heated anode is comparatively larger than the layer underneath the pre-heated anode. The underside of the side part which is facing towards the anodes which have been operating in the cell for two days or more has almost no frozen bath underneath it. The heat from the neighbouring anodes will contribute to the newly set anodes and reduce the amount of frozen layer on the sides that they are facing.

In the image of anode pair 1, it also seems like the slots of the normal anode are fairly more clogged than the pre-heated one. The degree of how open the slots are might be due to the production of the anodes but there could also be due to the pre-heating. From the IR-pictures one could see how the heat spread throughout the anodes after pre-heating. The heat was not able to spread as good to the part of the anode between the slots. This is probably due to the layer of air which is between the slots and this layer insulated and reduced the amount of heat being able to pass through. This was very prominent for the shorter amount of pre-heating time. Even though the heat did not pass the slot it still reaches the side wall of the slot and this could help reduce the amount of frozen bath forming and clogging the slots. Open slots are beneficial to the process since it reduces the resistance made by the gas bubbles. The slots will guide the gas bubbles out from the bath instead of accumulating underneath the anode and increasing the resistance.

The position in the cell will also have an impact on the formation of the frozen bath. As mentioned previously, the curvature of the metal will affect the temperature and the current pick-up rate in the anodes. Anode pair 2, where one anode was pre-heated for 2 hours, were placed in a more centre position than anode pair 1. While the pre-heated anode for anode pair 1 was more centre than the normal,

the opposite was the applied for anode pair 2. The non pre-heated anode was however placed further towards the centre compared to the pre-heated anode. Less frozen bath were found underneath the pre-heated one, so this could imply that the pre-heated had a positive affect on the formation of the frozen bath. There was used different cells for the different experiments, so the operating conditions of the cells could be different. Different cells will have some difference in the operating temperature, amount of carbon slag in the bath and stability. This will of course affect the disturbance to the cell as the anodes are replaced. Due to limited time, the experiments had to be performed at different cells.

7.6 Computed tomography

CT-analysis was performed on a total of 10 samples. 3 samples were taken from anode 7, 8, and 13 and 1 sample were taken from anode 12 Anode 12 had so much less frozen bath underneath it compared to the three other anodes so only two small samples were collected. Anode 7 was pre-heated for 1 hour, anode 12 was pre-heated for 2 hours while anode 8 and 13 were not pre-heated. A significant difference in the amount of frozen bath underneath the two different pairs could be observed.

By observing the CT-images, no clear difference was observed between the pre-heated anode and the non pre-heated anode pairs. For anode 7 and 8, most of the samples had a thin layer of frozen bath which had some minor cavities which probably comes from gas bubbles in it, but mainly it had a similar density. This was the layer that had frozen immediately when the anode was placed into the bath. After this layer, the frozen layer had a significantly number of cavities in it probably from gas development. Some slightly darker spots could be found in this layer as well indicating that there are areas with less density than the frozen bath. These darker spots are probably carbon. The spots are probably too bright to be pure carbon, but they could be carbon impregnated with bath or clusters made up of fine-grained carbon and bath. Most of the bath samples then had a section with less cavities and more evenly frozen bath but contained some darker spots. It seems that when the anodes are placed into the bath, a layer of frozen bath will freeze instantaneous under the anode. The next layer is thicker and will take longer to freeze. Then gas bubbles are able to create gas cavities in the frozen layer.

The samples gathered from anode 12 and 13 were thinner than from anode 7 and 8. The samples from anode 13 and 12 had the same thin layer which had frozen quickly on the bottom surface of the anode when it was placed into the bath. The next layer was similar in the way that it had more cavities. The number of darker spots were less in the samples from anode 12 and 13 compared to anode 7 and 8.

There might be difficult to distinguish the anode pairs from each other based

on the pre-heating technique used in this work. When observing the pictures taken with an IR-camera on the pre-heated anodes one could see how the pre-heating affected the bottom surface of the anodes. The area between the two slots were significantly less affected by the heat compared to the areas on the side of the slots. This was due to the slots creating a thin wall of air which reduces the transportation of heat across the slots. The heat is then unable to reach the centre of the bottom surface in the same way as the core position. Since the temperatures on the area between the two slots then won't be so different between the pre-heated and the normal anode, the difference between the composition and structure on the frozen bath between them won't be so different either. The samples collected of the frozen bath were mainly taken from the area between the two slots since that is where most of the frozen bath was made. This might make it difficult to observe a difference in the CT-images between the pre-heated and the normal.

To make a more certain decision of what the samples contained some more analysis would have to be performed. Analysing tools such as a scanning electron microscope (SEM) or an energy-dispersive X-ray spectroscope (EDS) would more easily reveal the chemical content. The samples would however need to be much smaller, which would be difficult with these samples. The samples might be a bit too large for the CT-scan to get a very clear image as well and they will change throughout since they were up to 15 cm long. There was however less frozen bath under the pre-heated ones even though they had different positions in the cell and a bit less bath in the slots could be seen.

7.7 Values in cell

The measurements of the air velocity and temperature of the air inside the cell showed an average velocity of 1.12 m/s and temperature of 147.7 °C. The measurements were performed at three different heights in each position in multiple cells. A total of 5 different cells were used to measure the values, but not every position was used in each cell. This was done because one wanted to measure under similar conditions. The conditions inside the cell vary between the cells. This can be conditions such as how big the opening is around the other anodes and the feeding hole. In this case, one wanted to find the velocity and the temperature of the air under conditions where most of the crust was intact. Since the feeding holes in Mosjøen are always open, this could affect the results to some degree.

The temperature values would probably be most affected by the opening in the crust. One of the tasks of the crust is to contain some of the heat inside the bath instead of releasing it. When there is an opening in the crust the thermal radiation will of course increase as well as the convection to the air. This might be the reason why the temperature is varying all the way from 130.5 °C to 164.5 °C. When the

anodes are really good packed with crust the heat transfer to the air is significantly reduced.

The air inside the cell is continuously sucked out of the cell through the fume collector in the hood on the inside of the cell. The power of the sucking is dependent on what is needed. If one of the removable covers on the cell is removed, some more power is needed to reduce the amount of gas being released to the pot hall. The measurements were performed by putting the pitot tube in between the removable covers to try and keep the power of the sucking as constant as possible. During the measurements the air velocity varied to a degree which is to be expected inside the cell.

Chapter 8

Concluding remarks

In the present work, the usage of surplus heat from the butts to pre-heat the carbon anodes were investigated. The butts were chosen because there is a constant supply of them and they have a high temperature. A pre-heating station using an anode container and insulating it with Rockwool mineral wool and heat resistant bricks and plates was used to keep the heat inside the system. Two butts were used to pre-heat one anode.

The pre-heating showed an increase in temperature inside the carbon anodes. After 4 hours, the temperature near the centre of the anode had on average increased from 5 °C to 140 °C. 4 hours of pre-heating seemed to be close to the optimal pre-heating time since the temperature started to flat out after 4 hours. A better insulated heating station could however decrease the heat loss to the ambient air, so the anodes could be pre-heated for a longer time and reach a higher temperature.

The current pick-up rates showed no statistically significant difference between the pre-heated anodes compared to non pre-heated anodes, but the pre-heating is still assumed to be beneficial. Having a higher initial temperature would lower the heat amount of heat that has to be taken from the surrounding electrolytic bath to heat the anode up to an operational temperature. In addition, it would reduce the disturbance to the cell and reduce the chance for the anode to crack. This is however difficult to estimate how it will affect the current pick-up rate of the cell. Previous studies have shown that the pre-heating have a significant improvement on the current pick-up rate at higher temperatures, how much other operations such as the interpolar distance or the disturbance from the anode change itself affects the pick-up rate is not known.

The calculations of the measured data showed that pre-heating the carbon anodes could result in an energy saving of up to 0.018 kWh/kg Al using the method applied in this work. This was the amount of energy saved in terms of reducing the amount of heat needed to heat up the anode to an operating temperature. For the world production of aluminium, it has the potential to save 1.16 TWh if all the anodes were pre-heated up to a temperature of 140 °C. Improvements to the pre-heating station could of course lead to a larger saving.

Finally, the formation of frozen bath under pre-heated anodes and non pre-heated anodes were investigated. For both 1 hour and 2 hours there was a significant difference in the amount of frozen bath formed under the pre-heated and the non pre-heated. The pre-heating seems to have an impact on the formation in specific areas underneath the anode as the anode pre-heated for 2 hours had significantly less frozen bath underneath compared to the other anodes. However, more experiments would need to be performed to draw a final conclusion regarding the impact from pre-heating. A CT-analysis of the samples were performed showing that the anodes in position 12 and 13 had less cavities and carbon within them compared to anode 7 and 8. No large difference within the pairs were observed as this would request some clearer image and the use of more analysing tools.

List of notations

A	: Area	[m^2]
α	: Absorptivity coefficient	[]
c_p	: Molar heat capacity	[J/K $\cdot$ mol]
E	: Emissive power	[W/m^2]
ε	: Emissivity	[]
F	: Faraday's constant	[C/mol]
η_e	: Stoichiomatric constant for aluminium	[]
η_{Al}	: Stoichiomatric constant for electrons	[]
G	: Irradiation	[W/m^2]
h	: Heat transfer coefficient	[W/m^2]
I	: Cell current	[A]
k	: Thermal conductivity	[W/m·K]
κ	: Electrical conductivity	[S/cm]
m	: Mass	[g]
μ	: Mean of population	[]
M_{Al}	: Molar mass aluminium	[g/mol]
q	: Heat energy	[W]
q''_x	: Heat flux	[W/m^2]
ρ	: Reflection factor	[]
R	: Resistivity	[Ω]
σ	: Stefan-Boltzmann constant	[W/$m^2 \cdot K^4$]
σ_M	: Standard error	[]
S	: Standard deviation for t-distribtion	[]
T	: Temperature	[K]
τ	: Transmission factor	[]
t	: Time	[s]
U	: Cell voltage	[V]
W_{el}	: Specific energy consumption	[kWh/kg]
X_{Al}	: Current efficiency for aluminium	[]
x	: Coordinates	[]
z	: Number of electrons	[]

Bibliography

[1] K. Grjotheim and H. Kvande. *Introduction to aluminium electrolysis : understanding the Hall-Héroult process*. eng. 2nd ed. Düsseldorf: Aluminium-Verlag, 1993. ISBN: 3870172339.

[2] B. Pedersen. *Aluminium*. Accessed 24.05.2019. Published 2018. URL: https://snl.no/aluminium.

[3] M. Holstad and T. Aanensen. *Elektrisitet, 2014 - Statistics Norway*. Accessed 12.06.2019. Published 2015. URL: https://www.ssb.no/energi-og-industri/statistikker/elektrisitet/aar/2015-12-22.

[4] The International Aluminium Institute. *Primary aluminium smelting energy intensity*. Accessed 03.03.2019. URL: http://www.world-aluminium.org/statistics/primary-aluminium-production/#data. 31.07.2018.

[5] J. Thonstad et al. *Aluminium electrolysis : fundamentals of the Hall-Héroult process*. eng. 3rd ed. Düsseldorf: Aluminium-Verlag, 2001. ISBN: 3870172703.

[6] A. Solheim. "Current Efficiency in Aluminium Reduction Cells: Theories, Models, Concepts, and Speculations." In: (2014).

[7] Shiva Prasad. "Studies on the Hall-Heroult Aluminium Electrowinning Process". In: *Journal of the Brazilian Chemical Society* (2000). URL: https://www.researchgate.net/publication/26363555.

[8] S. Kolås and T. Støre. "Bath temperature and AlF3 control of an aluminium electrolysis cell". In: *Control Engineering Practice* 17.9 (2009), pp. 1035–1043. ISSN: 0967-0661. DOI: https://doi.org/10.1016/j.conengprac.2009.03.008.

[9] F. Chevarin et al. “Substrate effect of coke particles on the structure and reactivity of coke/pitch mixtures in carbon anodes”. In: *Fuel* 183 (2016), pp. 123–131. ISSN: 0016-2361. DOI: https://doi.org/10.1016/j.fuel.2016.06.070.

[10] C. Cheung et al. “Characterization of Individual Anode Current Signals in Aluminum Reduction Cells”. In: *Industrial and Engineering Chemistry Reasearch* 52 (2013), pp. 9632–9644. DOI: https://doi.org/10.1021/ie400296u.

[11] P. Lavoie, M. Taylor, and J. Metson. “A Review of Alumina Feeding and Dissolution Factors in Aluminum Reduction cells”. In: *Metallurgical and Materials Transactions B* 47.4 (2016), pp. 2690–2696. ISSN: 1073-5615. DOI: https://doi.org/10.1007/s11663-016-0680-3.

[12] M. Tkac. “Porosity development in composite carbon materials during heat treatment”. PhD thesis. Norwegian University of Science et al., 2007. ISBN: 9788247122129.

[13] Felix Keller and Peter O. Sulger. *Anode baking : baking of anodes for the aluminium industry*. eng. Sierre, 2008.

[14] M. A. Engvoll. “Reactivity of anode raw materials and anodes for production of aluminium”. PhD thesis. Norwegian University of Science, Technology, Faculty of Natural Sciences, and Technology, Department of Chemistry, 2001. ISBN: 82471553882.

[15] W. Haupin and K. Kvande. “Thermodynamics of Electrochemical Reduction of Alumina”. In: *Light Metals* 2 (2000), pp. 160–165. DOI: https://doi.org/10.1002/9781118647851.ch22.

[16] M. W. Meier. “Cracking behaviour of anodes”. PhD thesis. Federal Institute of Technology, Zurich, 1996. ISBN: 3-9521028-1-4.

[17] M. Dupuis. *How to Limit the Heat Loss of Anode Stubs and Cathode Collector Bars in Order to Reduce Cell Energy Consumption*. Springer, Cham, 2019. ISBN: 978-3-030-05863-0. DOI: https://doi.org/10.1007/978-3-030-05864-7_67.

[18] W. E. Haupin. “Principles of Aluminum Electrolysis”. In: *Light Metals* 3-11 (1995), pp. 9632–9644. DOI: https://doi.org/10.1002/9781118647851.ch1.

[19] Y. Yurkov. *Refractories for Aluminium*. 2015. ISBN: 3319114417.

[20] Ali Jassim et al. “Studies on Anode Pre-Heating Using Individual Anode Signals in Hall-Héroult Reduction Cells”. In: *Light Metals 2016*. Ed. by Edward Williams. Cham: Springer International Publishing, 2016, pp. 623–628. ISBN: 978-3-319-48251-4. DOI: 10.1007/978-3-319-48251-4_105.

[21] O. Fortini et al. “Experimental Studies of the Impact of Anode Pre-Heating”. In: (2012), pp. 595–600. URL: https://ebookcentral.proquest.com/lib/ntnu/detail.action?docID=861728.

[22] D. Picard et al. “In Situ Evolution of the Frozen Layer Under Cold Anode”. In: *Light Metals 2019* (2019), pp. 795–802. DOI: https://doi.org/10.1017/978-3-030-05864-7_97.

[23] D. Picard et al. “Investigation of the Frozen Bath Layer under Cold Anodes”. In: *Metals* 7.9 (2017). ISSN: 2075-4701. DOI: 10.3390/met7090374. URL: http://www.mdpi.com/2075-4701/7/9/374.

[24] C. Nowicki and L. Gosselin. “An Overview of Opportunities for Waste Heat Recovery and Thermal Integration in the Primary Aluminum Industry”. In: *JOM* 64.8 (Aug. 2012), pp. 990–996. ISSN: 1543-1851. DOI: 10.1007/s11837-012-0367-4.

[25] R. Ødegård, A. Solheim, and K. Thovsen. “Current Pickup and Temperature Distribution in Newly Set Prebaked Hall-Héroult Anodes”. In: *Essential Readings in Light Metals: Volume 2 Aluminum Reduction Technology*. Ed. by Geoff Bearne, Marc Dupuis, and Gary Tarcy. Cham: Springer International Publishing, 2016, pp. 555–561. ISBN: 978-3-319-48156-2. DOI: 10.1007/978-3-319-48156-2_82.

[26] Q. Wang, B. Li, and M. Fafard. “Effect of Anode Change on Heat Transfer and Magneto-hydrodynamic Flow in Aluminum Reduction Cell”. In: *JOM* 68.2 (Feb. 2016), pp. 610–622. ISSN: 1543-1851. DOI: 10.1007/s11837-015-1714-z.

[27] F. P. Incropera et al. *Principles of heat and mass transfer*. eng. 7th ed. Singapore: Wiley, 2013. ISBN: 9780470646151.

[28] G. E. Miller. *Biomedical Transport Processes*. 3rd ed. Academic Press, pp. 937–993. ISBN: 978-0-12-374979-6.

[29] Encyclopædia Britannica. *Thermal radiation*. Accessed 03.06.2019. Published 2018. URL: https://www.britannica.com/science/thermal-radiation.

[30] M. Mayil, G. Keser, and F. N. Pekiner. *CBCT images of anatomic landmarks in maxillofacial region*. Yerkure Tanitim ve Yayincilik Hizmetleri A.S., 2014. DOI: 10.5455/musbed.20140814010458.

[31] W. C. Scarfe and C. Angelopoulos. *Maxillofacial Cone Beam Computed Tomography: Principles, Techniques and Clinical Applications*. Springer International Publishing, 2018. ISBN: 3-319-62061-4.

[32] A. Saar. *Principle of CBCT*. Accessed 21.05.2019. Published 2014. URL: https://commons.wikimedia.org/wiki/File:Cone_Beam_CT_principle.png.

[33] C. Woodford and C. Phillips. *Numerical Methods and Worked Examples: Matlab Edition*. Dordrecht: Springer Netherlands, 2012, pp. 71-96. ISBN: 9789400713659. DOI: 10.1007/978-94-007-1366-6_4.

[34] R. E. Walpole et al. *Probability and statistics for engineers and scientists*. 9th ed. Pearson Education, 2016. ISBN: 978-0-321-62911-1.

[35] H. M. Wadsworth. *Handbook of statistical methods for engineers and scientists*. 2nd ed. McGraw-Hill, 1998. ISBN: 007067678X.

[36] W. L. Hays. *Statistics*. 5th ed. Harcourt Brace, 1994. ISBN: 0030744679.

[37] M. J. Bland and D. G. Altman. *Statistics Notes: Measurement error*. British Medical Journal Publishing Group, 1996. DOI: 10.1136/bmj.313.7059.744.

[38] D. Kernler. *A visual representation of the Empirical (68-95-99.7) Rule based on the normal distribution*. Accessed 15.06.2019. Published 2014. URL: https://commons.wikimedia.org/wiki/File:Empirical_Rule.PNG.

[39] Skbkekas. *Plot of the density function for several members of the Student t family*. Accessed 15.06.2019. Published 2010. URL: https://commons.wikimedia.org/wiki/File:Student_t_pdf.svg.

[40] B.S. Everitt and A. Skrondal. *The Cambridge Dictionary of Statistics*. 4th ed. Cambridge University Press, New York, 2010. ISBN: 978-0-521-81099-9.

[41] National Institute of Standards and Technology. *NIST-JANAF Thermochemical Tables - Carbon*. Accessed 27.04.2019. URL: https://janaf.nist.gov/tables/C-002.html.

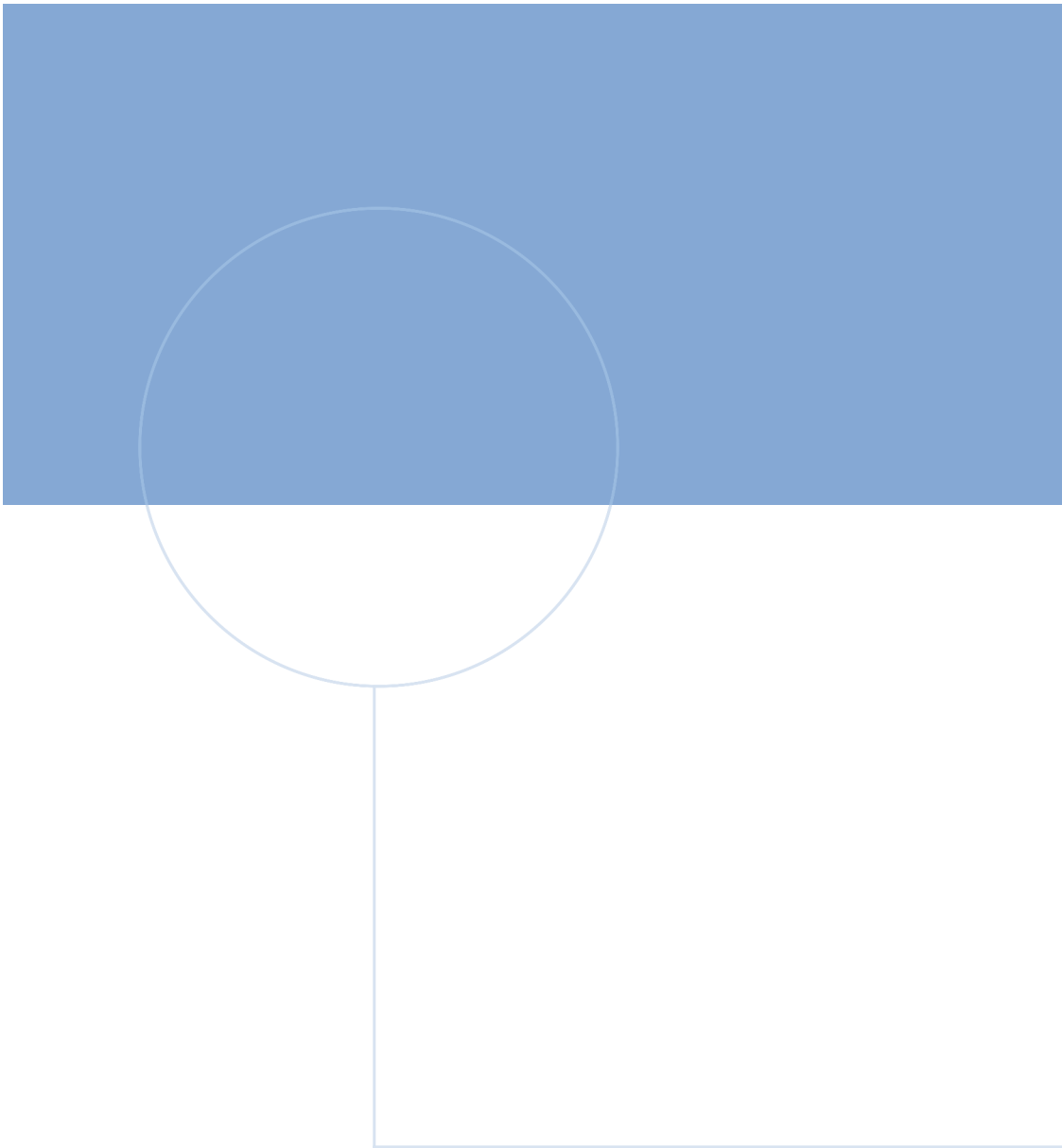

NTNU
Norwegian University of
Science and Technology